

**Effect of Nitriding Temperature on Duplex Stainless Steel**

By

Nurhafiza Bt Mohd Ghazi

(11705)

Project Dissertation submitted in partial fulfillment of  
the requirements for the  
Bachelor of Engineering (Hons)  
(Mechanical Engineering)

SEPTEMBER 2011

Universiti Teknologi PETRONAS,  
Bandar Seri Iskandar,  
31750 Tronoh,  
Perak Darul Ridzuan.

**CERTIFICATION OF APPROVAL**

**Effect of Nitriding Temperature on Duplex Stainless Steel**

By

Nurhafiza bt Mohd Ghazi

(11705)

A project dissertation submitted to the

Mechanical Engineering Programme

Universiti Teknologi PETRONAS

In partial fulfilment of the requirement for the

BACHELOR OF ENGINEERING (Hons)

(MECHANICAL ENGINEERING)

Approved by,



---

(AP. Dr. Patthi bin Hussain)

UNIVERSITI TEKNOLOGI PETRONAS

TRONOH, PERAK

September 2011

### **CERTIFICATION OF ORIGINALITY**

This is to certify that I am responsible for the work submitted in this project, that the original work is my own except as specified in the references and acknowledgements, and that the original work contained herein have not been undertaken or done by unspecified sources or persons.



---

**NURHAFIZA BT MOHD GHAZI**

## ABSTRACT

This project discussed about the project titled Effect of Nitriding Temperature of Duplex Stainless Steel. This report consisted of the project's background, objectives, and problem statements, scope of work, literature review, methodology or the flow of the project, result & discussion and last but not least the conclusion. In this work the author report a study of the surface modification and hardness improvement of duplex stainless steel (DSS) nitride by nitrogen gaseous have been conducted in a horizontal tube furnace at four different temperatures. Nitriding is one of the traditional thermochemical treatments for surface engineering that can be utilized in order to harden the duplex stainless steel surface to resist any failure. In order to conduct the nitriding process, it is crucial to highlight the important of its variables such as time, temperature and gas velocity. This is because, all these variables have contribute each significance effect especially in terms of the nitriding process itself and the effect of mechanical properties of the samples. However, for this project, the author have investigated and identified the effect of utilizing variations of nitriding temperatures in order to improve and enhance the strength and hardness of the duplex stainless steel. Therefore, the result of before and after being nitride of the samples have been observed for different temperatures. This objective have been achieved by a series of laboratory tests such as metallographic study, and XRD examination and assessment of the sample's hardness using Vickers Microhardness Testing after the treatment were performed to examine the result of the treatment. The sample's microstructures have been examined by using Scanning Electron Microscopy with Energy Dispersive X-ray Spectrometry (SEM-EDX). Results of these laboratory tests have been used to analyze both of the strength and microstructures of the samples. The result showed that there is markedly effect of nitriding temperatures to both strength and microstructures of samples. As the nitriding temperature increased, the hardness of samples also increased. Last but not least, the objectives of this work have been achieved successfully.

## ACKNOWLEDGMENT

First and foremost, my deepest gratitude to Allah SWT, the Lord of Universe for his blessings and guidance in various aspects for me to accomplish my final year project entitled 'Effect of Nitriding Temperature on Duplex Stainless Steel'. Special thanks to my parents and family members for their continuous support and encouragement towards me all this while in completing this project.

Secondly I am heartily thankful to my supervisor, AP Dr. Patthi bin Hussain, who has supported and encouraged me throughout my thesis with his patience and knowledge whilst allowing me the room to work in my own way. His invaluable help of constructive comments and suggestions throughout the experimental and thesis works have contributed to the success of this research.

I also want to thank Mr. Askar Triwiyanto for his guidance and assistance in preparation of samples and conducting nitriding. He has been a great help during the whole experimental process. A high appreciation to all Mechanical Department technicians especially Mr. Faizal, Mr. Mahfuz, Mr. Paris, Mr. Irwan, Mr. Anuar and Mr. Shaiful for their assistance in all the experiments carried out to complete this project. The project would never been a success without support and technical assistance from all of them.

Finally, thank you to Mechanical Engineering Department, Examiners, and Coordinators of the Final Year Project for making this program a success. They have been very helpful and considerate throughout this whole project. Last but not least, my most heartfelt appreciation to all parties involved, for their contribution, guidance, as well as significant support given until the completion of this research. Without all of them, I would not have been able to accomplish and meet the objective of this project in total.

Hopefully this project will provide the readers with more knowledge and understanding towards wear behaviour and wear mechanisms at rail track.

Thank you,

Nurhafiza Bt Mohd Ghazi

Mechanical Engineering Department

## Table of Contents

CERTIFICATION OF APPROVAL .....	i
CERTIFICATION OF ORIGINALITY .....	ii
ABSTRACT .....	iii
ACKNOWLEDGMENT .....	iv
LIST OF FIGURE .....	vii
LIST OF TABLE .....	viii
ABBREVIATIONS AND NOMENCLATURES .....	ix
CHAPTER 1: INTRODUCTION .....	1
1.1 Project Background.....	1
1.2 Problem Statement.....	2
1.3 Objective and Scope of Study.....	2
CHAPTER 2: LITERATURE REVIEW.....	4
2.1 The Duplex Family - Development History, Chemistry, Applications.....	4
2.1.2 Duplex Stainless Steels .....	4
2.1.1 LDX 2101 .....	5
2.2 Chemical Composition of Duplex Stainless Steel and Role of Alloying Elements.....	6
2.2.1 Chemical composition of Duplex Stainless Steels (DSS).....	6
2.2.2 The role of alloying elements in duplex stainless steels .....	7
2.3. Metallurgy of Duplex Stainless Steels (DSS).....	8
2.3.1 Microstructure and Concentration Profiles.....	8
2.3.2 Element Partitioning - Substitutional Element of Nitrogen .....	10
2.3.3 Effect of Cooling Time of Duplex Stainless Steel .....	11
2.4 CONCEPT OF NITRIDING.....	12
2.4.1 Previous Studies on High Temperature Gas Nitriding (HTGN).....	13
CHAPTER 3: METHODOLOGY .....	21
3.1: Project Flow Chart.....	21
3.2 Procedures.....	22
3.2.1 Research Methodology .....	22
3.2.2 Material Acquisition .....	22
3.2.3 Sample Preparation .....	22

3.2.4 Nitriding Process.....	24
3.3 X-ray Diffraction Analysis.....	27
3.4 Microstructure Examination.....	29
3.5 Hardness Test.....	31
3.5.1 Vickers Test Method.....	32
3.6 Gantt Chart.....	33
CHAPTER 4: RESULT AND DISCUSSION.....	35
4.1 Introduction.....	35
4.2 Mass/weight differences before and after nitriding.....	35
4.3 Vickers Microhardness.....	36
4.4 Microstructure and morphology Analysis.....	38
4.4.1 SEM – Microstructure Images on surface layer.....	39
4.4.2 Microstructure Images by Optical microscope (OM).....	42
4.4.3 EDX Analysis – Line scan nitrogen profile .....	45
4.4.4 EDX Analysis - Area Analysis .....	47
4.4.5 EDX Analysis - Spot Analysis.....	51
4.4.6 X-ray Diffraction Analysis .....	57
CHAPTER 5: CONCLUSION & RECOMMENDATION .....	60
5.1 Conclusion.....	60
5.2 Recommendation.....	61
REFERENCES .....	62
APPENDIX.....	65

## LIST OF FIGURE

Figure 1: Duplex stainless steels have a two-phase microstructure of austenite and ferrite grains .....	5
Figure 2: Typical microstructure of DSS wrought (a) and cast (b) form.....	9
Figure 3: Section through the Fe-Cr-Ni ternary phase diagram at 68% iron and the schematic effect of nitrogen additions is shown in darker region.....	10
Figure 4 : Variation of austenite content with cooling time at various nitrogen content, Ferrite grain size as a function of cooling time at various nitrogen content	12
Figure 5: Schematic illustration of the gas nitriding equipment .....	14
Figure 6: Section through the solution nitrided case of the duplex stainless steel. The microstructural constituents are: austenite (A), ferrite (F), nitride ( $M_2N$ ).....	16
Figure 7: Hardness as a function of the depth below the surface after HTGN treatment for 10 hr .....	17
Figure 8: Phase diagram of grade 1.4501 versus nitrogen content .....	18
Figure 9: X-ray diffraction result of plasma nitrided of duplex stainless steel.....	19
Figure 10: Project's flow chart .....	21
Figure 11: Electrical Discharge Machine (EDM).....	23
Figure 12: Grinding Process .....	24
Figure 13: Lenton Horizontal tube furnace.....	25
Figure 14: Flow meter.....	25
Figure 15: Oxygen indicator .....	26
Figure 16: Scrubber cone flask .....	26
Figure 17: Ultrasonic cleaner.....	26
Figure 18: Alumina boat .....	27
Figure 19: The reflection of an X-ray beam by the (hkl) planes of a crystal [14] .....	28
Figure 20: X-ray Diffraction Machine [14] .....	29
Figure 21: Microstructure examination using optical microscope .....	29
Figure 22: Scanning electron microscope.....	30



Figure 23: a) Fry reagent, b) Applying etching solution, c) Applying ethanol, .....	31
Figure 24: a) Vickers Hardness Equipment .....	32
Figure 25: Percentage weight difference vs Nitriding temperature for unnitrided sample and nitrided samples .....	36
Figure 26: Hardness profile over distance from the surface to the minimum distance of the core of the steels .....	37
Figure 27: SEM microstructure images at various temperatures : unnitrided, 950°C, 1000°C, 1050°C and 1100°C .....	41
Figure 28: OM images of unnitrided sample and nitrided samples at temperatures of 950°C, 1000°C, 1050°C and 1100°C.....	42
Figure 29:Nitrogen profile at temperature of: a) 950°C, b)1000°C, c)1050°C and d) 1100°C .....	47
Figure 30: Image and qualitative result of unnitrided sample .....	48
Figure 31: Image and qualitative result of nitrided at 950°C.....	49
Figure 32: Image and qualitative result of nitrided at 1000°C.....	49
Figure 33: Image and qualitative result at 1050°C .....	50
Figure 34: Image and qualitative result of nitrided at 1100°C.....	50
Figure 35: a) Image of spectrum 3 and spectrum 4, b) Qualitative result .....	52
Figure 36: a) Image at spectrum 6 and spectrum 7, b) Qualitative result.....	53
Figure 37: a) Image of spectrum 2 and spectrum 1, b) Qualitative result .....	54
Figure 38: a) Image at spectrum 1 and spectrum 3 .....	55
Figure 39: a) Image at spectrum 3 and spectrum 5, b) Qualitative result.....	56
Figure 40: XRD patterns for duplex stainless steel of unnitrided sample and nitrided samples.....	59

#### **LIST OF TABLE**

Table 1: Theory or general chemical composition in % of LDX 2101 .....	6
Table 2: The milestones of FYP I project research.....	33
Table 3: The milestone of FYP II project research.....	34
Table 4: Weight of samples on particular nitriding temperatures.....	36

Table 5: Microhardness data of unnitrided and nitrided samples .....	37
Table 6: Quantitative result.....	48
Table 7: Quantitative result.....	49
Table 8: Quantitative result.....	49
Table 9: Quantitative result.....	50
Table 10: Quantitative result.....	50
Table 11: Spectrum 3 of austenite phase .....	52
Table 12: Spectrum 4 of ferrite phase.....	52
Table 13: Spectrum 6 on austenite phase.....	53
Table 14: Spectrum 7 on ferrite phase .....	53
Table 15: Spectrum 2 on austenite phase.....	54
Table 16: Spectrum 1 of ferrite phase.....	54
Table 17: Spectrum 1 on austenite phase.....	55
Table 18: Spectrum 3 on ferrite phase .....	55
Table 19: Spectrum 3 of austenite phase .....	56
Table 20: Spectrum 5 at ferrite phase .....	56

## **ABBREVIATIONS AND NOMENCLATURES**

DSS – Duplex Stainless Steel  
 LDX – Lean Duplex Stainless Steel  
 OM – Optical Microscope  
 XRD – X-Ray Diffractometer  
 SEM – Scanning electron microscope  
 EDX- Energy Dispersive X-ray Spectrometer  
 HTGN – High Temperature Gas Nitriding  
 FCC – face-centered cubic  
 BCC – body-centered cubic  
 EDM – Energy Discharge Machine

## **CHAPTER 1: INTRODUCTION**

### **1.1 Project Background**

First and foremost, the protection of material surfaces from unreceptive environments and rigorous operating conditions is of great technical awareness and economic necessity in the mechanical engineering industry. This is due to the surface and subsurface properties of materials which establish their performance. Therefore, the requirements of high hardness, with improved wear, corrosion and fatigue properties can be gained by surface modifications using nitriding process. Nitriding is one of diffusion treatments applied to the surface of machine parts, tools, and other metallic objects to enhance their surface hardness and improve the mechanical properties.

For this time, the author have conducted a gas nitriding at high temperature process (HTGN) of duplex stainless steel at different temperatures whereby nitrogen is diffuse into the surface of a solid ferrous alloy by hold the metal at four different temperatures with constant time and constant pressure in contact with a nitrogenous gas. The material that has been used for this project is duplex stainless steel and to be more specific it is a duplex stainless steel from type of Lean Duplex, LDX 2101. Duplex stainless steels are called “duplex” because they have a two-phase microstructure consisting of grains of ferritic and austenitic stainless steel. For instance, the name of 2101 comes from typical chemical composition of 21% of chromium and 1 to 1.5% of nickel. The author has investigated and examined the effect of utilizing variations values of nitriding temperatures in term of hardness profile and any microstructure changes.

Therefore, in order to identify all these samples evolutions, the author was using Lenton Horizontal Tube Furnace to conduct the gas nitriding process, X-Ray Diffractometer (XRD), Scanning Electron Microscope with Energy-Dispersive X-Ray Spectroscopy, SEM-EDX, Optical Microscope, OM and Vickers Microhardness on the samples.

## **1.2 Problem Statement**

Duplex Stainless Steel is used in industry since it has a two-phase microstructure consisting of grains of ferritic and austenitic stainless steel. It has a good corrosion resistance with high strength but it is also brittle. So, by nitriding process, it can improve the strength and hardness of the steel. We need to improve the hardness and toughness of the material in order to improve the durability of the tools so that it will have longer time frame. Nitriding will involve in heating the samples at high temperature with nitrogenous gas that will be diffused to the surface of each samples. Besides, we are required to identify and investigate the effect of using variations value of nitriding temperatures to the samples in terms of its hardness profile, and microstructure changes. Not to forget, while the author varied the temperatures values, the time constraint used is constant in six hours for all the experiments.

## **1.3 Objective and Scope of Study**

The objective of this project is divided into two significance purposes which are:

- To improve the hardness and strength by performing nitriding process (HTGN process)
- To observe and compare of any microstructure changes of the samples before and after been nitrided.

The Vickers Microhardness testing has been conducted as following and referring to the standard of ASTM E-92. The author followed and referred the test procedure. Although empirical in nature, can be correlated to tensile strength for many metals, and is an indicator of the material's hardness profile.

On top of that, scope of study of this project is mainly in the form of laboratory experiments. This project cover on the conducting the gas nitriding at high temperature on the duplex stainless steel or for this case using LDX 2101, identify the effect of nitriding temperatures in terms of the hardness and microstructure behaviour of the samples before and after nitriding.

The conventional high temperature gas nitriding process (HTGN) has been conducted in a horizontal tube furnace for four different temperatures.

Therefore, the mechanical properties included hardness and physical properties of the material are expected to be improved. On top of that, the microstructure changes of before and after nitriding, and the hardness have been determined by analyzing the SEM micrograph, XRD Analysis and Vickers Microhardness Testing. For other relevant work, SEM-EDX can be used to identify and find out of which elements different parts of a sample contains. As far as the author concern, in order to identify the present of nitrogen diffused at the surface of the samples after been nitrided, the author can utilize the SEM-EDX machine. [1] Not to forget, all these observation and identification highlighted the significance relationship of utilizing variations of nitriding temperatures which could affect the result compiled.

After the required data is acquired, the project is considered as complete. The result obtained can be used for future work.

## **CHAPTER 2: LITERATURE REVIEW**

### **2.1 The Duplex Family - Development History, Chemistry, Applications**

Throughout chapter 2, the materials reviewed and the information related to the materials involved will be discussed deeper. It is important to know the details about materials being researched and the process involved from the beginning until the end.

#### **2.1.2 Duplex Stainless Steels**

Duplex stainless steels are a mixture of Body-Centered Cubic (BCC) ferrite and Face-Centered Cubic (FCC) austenite crystal structures. The percentage each phase depends on the composition and heat treatment. Most duplex stainless steels are intended to contain around equal amounts of ferrite and austenite phases in the annealed condition. The primary alloying elements are chromium and nickel. As duplex stainless steels are consisting of austenitic-ferritic, it combines many of the beneficial properties of ferritic austenitic steels. Due to their high content of chromium and nitrogen, and often also molybdenum, these steels offer good resistance to local and uniform corrosion. The duplex microstructures contribute to their high strength and high resistance to stress corrosion cracking. Duplex steels also have good weldability. In industry, there are four distinct groups of duplex stainless which differ of its containing alloys elements [1]. There are:

- i. Lean duplex steel, low-alloyed (Ni,Mo), like e.g. 1.4162 (LDX 2101®), 1.4362 (2304)
- ii. Standard duplex steels, normal-alloyed (Ni,Mo), like e.g. 1.4462 (2205), 1.4460
- iii. Super duplex steels, high-alloyed (Ni,Mo,N), like e.g. 1.4410 (SAF 2507®), 1.4501
- iv. Hyper duplex steels, very high-alloyed (Ni,Mo,N,Co), like e.g. Sandvik SAF 2707 HD®, Sandvik SAF 3207 HD®

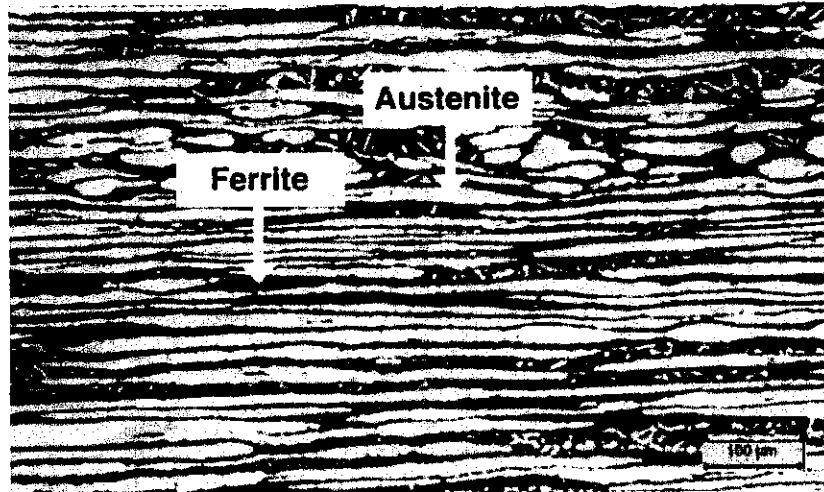


Figure 1: Duplex stainless steels have a two-phase microstructure of austenite and ferrite grains [1]

The picture shows the yellow austenitic phase as “islands” surrounded by the blue ferritic phase. When duplex stainless steel is melted it solidifies from the liquid phase to a completely ferritic structure. As the material cools to room temperature, about half of the ferritic grains transform to austenitic grains (“islands”). [1]

### 2.1.1 LDX 2101

For this project, the author will use a duplex stainless steel. As far as concern, duplex stainless steels are consisting of several types. The examples are Duplex 2205 and Duplex 2507. For this instance, a new patent correspond to the type S32101 DSS has been developed recently and the author used LDX 2101 as samples for this nitriding experiment. Lean duplex stainless (LDX) steel 2101 is a new patent of duplex stainless steel and it has its own grade of steel according to standards. However, the author will conduct the morphology and chemical composition analysis in order to determine the precision of this material itself whether it is in line with the general chemical composition of this grade of LDX 2101. The general or theory chemical composition of duplex stainless steel in type of LDX 2101 which are [5]:

The general and standard chemical composition (%) of LDX 2101 is:

Table 1: Theory or general chemical composition in % of LDX 2101 [5]

<b>Alloy</b>	<b>Min (%)</b>	<b>Max (%)</b>
Chromium, Cr	21.00	22.00
Nickel, Ni	1.35	1.70
Manganese, Mn	4.00	6.00
Molybdenum, Mo	0.10	0.80
Nitrogen, N	0.20	0.25
Carbon, C	-	0.040
Silicon, Sc	-	1.00
Copper, Cu	0.10	0.80
Phosphorus, P	-	0.040
Sulfur, S	-	0.030
Iron, Fe	Balance	

Last but not least, LDX 2101 are been used widely in industry. Numbers of application of LDX 2101 stainless steel are been used in general purpose stainless steel applications, for chemical process pressure vessels, piping and heat exchangers, storage tanks, water treatment, pulp and paper mill equipment and water heater tanks. [5]

## 2.2 Chemical Composition of Duplex Stainless Steel and Role of Alloying Elements

### 2.2.1 Chemical composition of Duplex Stainless Steels (DSS)

It is generally accepted that the favorable properties of the duplex stainless steels (DSS) can be achieved for phase balances in the range of 30% to 70% ferrite and austenite. However, duplex stainless steel is most commonly considered to have roughly equal amounts of ferrite and austenite and according to current commercial production which slightly favoring the austenite for best toughness and processing characteristics. The interaction of the major alloying elements such as chromium, nitrogen, molybdenum, and nickel are quite difficult [2].



Besides the phase balance, the second major concern with DSS and their chemical composition is the formation of intermetallic phases at elevated temperatures. Sigma and chi phases form in high chromium, high molybdenum stainless steels and precipitate preferentially in the ferrite. Therefore, the addition of nitrogen significantly delays formation of these phases. It is critical to have sufficient nitrogen present in solid solution [1, 2, 4].

## **2.2.2 The role of alloying elements in duplex stainless steels**

### **i) Nitrogen**

Nitrogen increases the pitting and crevice corrosion resistance of duplex stainless steels. It also substantially increases their strength and, in fact, it is the most effective solid solution strengthening element and a low-cost alloying element. The improved toughness of nitrogen bearing duplex stainless steels is due to their greater austenite content and reduced intermetallic content. Nitrogen does not prevent the precipitation of intermetallic phases but delays the formation of intermetallics enough to permit processing and fabrication of the duplex grades. It is also reported that increasing the nitrogen level actually reduces the risk of nitride formation. However, this may appear contradictory, but it is due to an increase in austenite and so a reduction in the distance between austenite islands. Another important property of nitrogen is its ability to stabilize duplex alloys against the precipitation of intermetallic phases such as sigma and chi by reducing Cr partitioning. Nitrogen is added to highly corrosion resistant duplex stainless steels that contain high chromium and molybdenum contents to offset their tendency to form sigma phase. Nitrogen is a strong austenite former and can replace some nickel in the austenitic stainless steels. Nitrogen reduces the stacking fault energy and increases the work hardening rate of austenite. It also increases the strength of austenite by solid solution strengthening. The addition of C and N strengthens both ferrite and austenite by dissolving at interstitial sites in the solid solution. And yet, as carbon is undesirable in stainless steel which can cause sensitization, the addition of nitrogen is preferred as have been mentioned before that nitrogen is a strong austenite stabiliser and its addition to duplex stainless steel suppresses austenite dissolution and encourages austenite reformation in the heat affected zone [1, 2].

#### i) Chromium

Chromium is a ferrite former, meaning that the addition of chromium promotes the body centered cubic structure of iron. At higher chromium contents, more nickel is needed to form an austenitic or duplex structure. Higher chromium also promotes the formation of intermetallic phases. It is at least 20% of chromium in duplex grades. Chromium also increases oxidation resistance at elevated temperatures [1, 2].

#### ii) Molybdenum

Molybdenum acts to support chromium in providing pitting corrosion resistance to stainless steels. It is a ferrite former and also increases the tendency of stainless steels to form detrimental intermetallic phases. Molybdenum restricted to less than about 4% in duplex stainless steels [1, 2]

#### iv) Nickel

Nickel is an austenite stabilizer, which promotes a change of the crystal structure of stainless steel from body-centered cubic (ferritic) to face-centered cubic (austenitic). Ferritic stainless steels contain little or no nickel, duplex stainless steels contain low to intermediate amount of nickel such as 1.5 to 7%. The addition of nickel delays formation of detrimental intermetallic phases but is far less effective than nitrogen in delaying their formation in duplex stainless steels. The face-centered cubic structure is responsible for the excellent toughness of the austenitic stainless steels. Its presence in about half of the microstructure of duplex grades greatly increases their toughness relative to ferritic stainless steels [1, 2].

### **2.3. Metallurgy of Duplex Stainless Steels (DSS)**

#### **2.3.1 Microstructure and Concentration Profiles**

During solidification, duplex first solidifies as ferrite. As temperature decreases, austenite develops. For cast duplex, a structure of austenite islands in a ferrite matrix can be observed. For wrought alloys, the microstructure has morphology of laths of austenite in a ferrite matrix. Figure 2 shows the typical microstructure of DSS in wrought (a) and cast (b) form [1, 2, and 4].

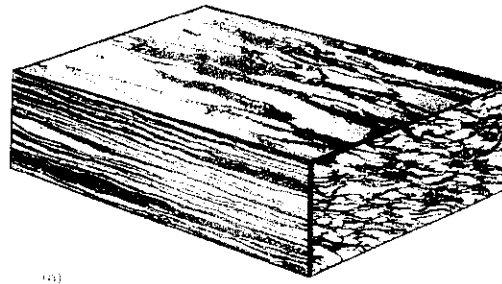
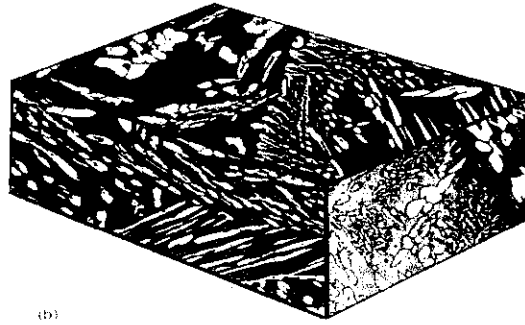


Figure 2: Typical microstructure of DSS wrought (a) and cast (b) form



The iron-chromium-nickel ternary phase diagram is a roadmap of the metallurgical behaviour of the duplex stainless steels. A section through the ternary at 68% iron as shown in figure 3 as below, illustrates that these alloys solidify as ferrite ( $\alpha$ ), some of which then transforms to austenite ( $\gamma$ ) as the temperature falls to about 1000°C (1832°F) depending on alloy composition. There is little further change in the equilibrium ferrite-austenite balance at lower temperatures. The effect of increasing nitrogen is also shown in figure 3. Thermodynamically, because the austenite is forming from the ferrite, it is impossible for the alloy to go past the equilibrium level of austenite. However, as cooling proceeds to lower temperatures, carbides, nitrides, sigma, and other intermetallic phases are all possible microstructural constituents [1, 3]

The ferrite/austenite phase balance in the microstructure can be predicted with multivariable linear regression as follows [1]:

$$\text{Cr}_{\text{eq}} = \% \text{Cr} + 1.73 \% \text{Si} + 0.88 \% \text{Mo}$$

$$\text{Ni}_{\text{eq}} = \% \text{Ni} + 24.55 \% \text{C} + 21.75 \% \text{N} + 0.4 \% \text{Cu}$$

$$\% \text{ Ferrite} = -20.93 + 4.01 \text{Cr}_{\text{eq}} - 5.6 \text{Ni}_{\text{eq}} + 0.016 \text{T}$$

Where T (in degree celcius) is the annealing temperature ranging from 1050-1150°C and the elemental compositions are in wt%. The goal of maintaining the desired phase balance in a duplex stainless steels is achieved primarily by adjusting chromium, molybdenum, nickel and nitrogen contents, and then control by thermal history[1, 2].

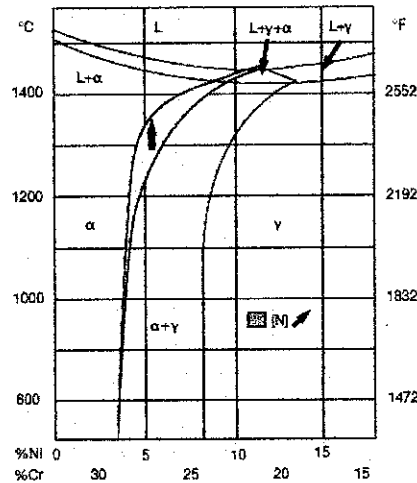


Figure 3: Section through the Fe-Cr-Ni ternary phase diagram at 68% iron and the schematic effect of nitrogen additions is shown in darker region [1].

Another beneficial effect of nitrogen, evidenced in Figure 3 is that it raises the temperature at which the austenite begins to form from the ferrite. This increases the rate of ferrite to austenite transformation. Therefore, even at relatively rapid cooling rates, the equilibrium level of austenite can almost be reached. Nitrogen is used as an alloying element to increase corrosion resistance. It also hinders the intermetallic formation and but also causes austenite to appear in higher temperatures. Formation of austenite in higher temperatures hinders intermetallic formation and segregation of the corrosion resistive elements. However, the disadvantage with nitrogen is that its solubility to ferrite is limited and thus excessive usage of it can lead to formation of pores or nitride precipitation [1, 2].\

### 2.3.2 Element Partitioning - Substitutional Element of Nitrogen

Several studies [1,2 and 3] have revealed the composition of the phases and resultant partition coefficients in solution annealed product and have demonstrated that, with exception of nitrogen, the partition coefficients for a given element do not vary significantly between alloys, in spite of wide range of compositions investigated.

This is due to the solubility limits for these elements not being exceeded. All agree that the ferrite is enriched in P, W, Mo, Si and Cr and the austenite in N, Ni, Cu, and Mn.

The partition coefficient for nitrogen is vary distinctly between alloys and is highly dependent on composition. In particular, Cr and Mn increase nitrogen solubility. Not only that, nitrogen partition coefficient is controlled by temperature. As during solution anneal, even though the solubility of nitrogen in ferrite may increase a little, the volume fraction of austenite decrease markedly. This leads to enrichment of nitrogen in the remaining austenite and so nitrogen partitioning is increased. Moreover, it has been observed that the nitrogen content is highest next to ferrite which is austenite interface and just within the austenite due to phase boundary displacement. However, on cooling, austenite formation occurs and the ferrite becomes rapidly saturated with nitrogen, with the excess nitrogen diffusing into the austenite, with 0.03-0.05% being the equilibrium solubility limit in ferrite at ambient temperatures [1].

### **2.3.3 Effect of Cooling Time of Duplex Stainless Steel**

As the author will conduct the high temperature gas nitriding process of duplex stainless steel, the samples will be heated until temperature 1100°C, 1050°C, 1000°C and 950°C in the nitrogen inert environment before the samples are allow to be cool in environment with slow cooling. From the research made by E. Erisir from University of Kocaeli, Turkey, in his investigations of samples cooled at 0.003 K/s which is slow cooling process, intermetallic phases were observed with ferrite and austenite grains [8]. The precipitates were appeared within grains or at grain boundaries of the ferrite, but not within the austenite. According to studies at literature [1,3 and 8], the precipitation of intermetallic phases in austenite is very sluggish due to the ferrite forming elements Cr and Mo and takes thousands of hours.

From figure 4 as below, stated the relationship between various austenite content in 22% Cr duplex stainless steel with cooling time at various nitrogen content and the relationship of ferrite grain size in the same type of duplex stainless steel with cooling time at numbers of nitrogen content [8].

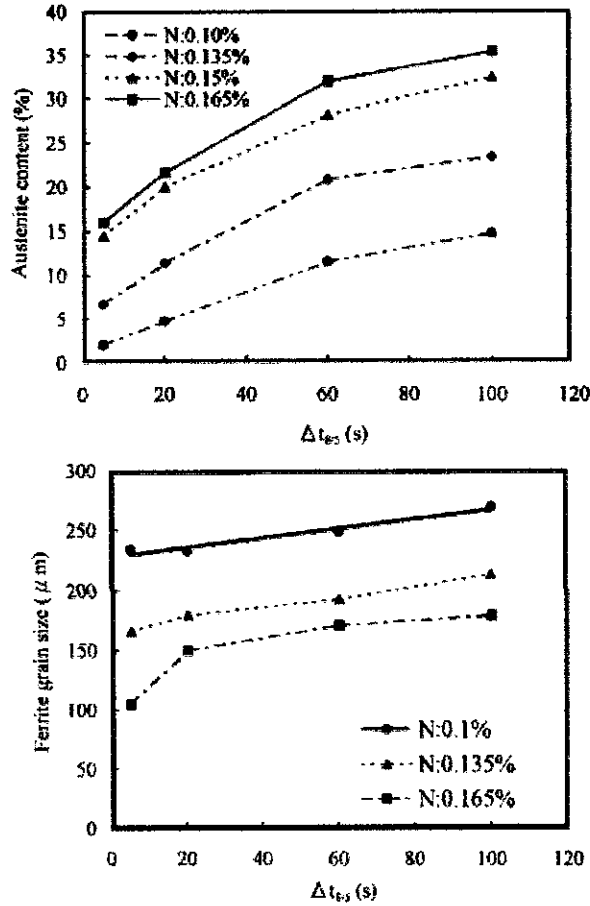


Figure 4 : Variation of austenite content with cooling time at various nitrogen content, Ferrite grain size as a function of cooling time at various nitrogen content

From figure 4, [8] it can be seen that the austenite content significantly increases with increasing nitrogen content at any given cooling time. While, from the same figure, it also shows the ferrite grain size reduction with decreasing cooling time and increasing nitrogen content. However, the effect of nitrogen content on the grain size is more evident than that of cooling time.

## 2.4 CONCEPT OF NITRIDING

Generally, nitriding is a surface-hardening heat treatment which introduces nitrogen into the surface of duplex stainless steels at certain temperature range [20]. Besides, nitriding also does not engage heating into the austenite phase field and a consequent quench to structure martensite. Not only that, nitriding can be consummate with a minimum of distortion and with tremendous dimensional control. Process method of nitriding is divided into three types of methods which are gas which using horizontal

tube furnace or fluidized bed. Next, using liquid or in other word is salt bath. The other common nitriding method is plasma which using ion nitriding [20].

There are several principal reasons of conducting nitriding which are [20]:

- To obtain high surface hardness
- To increase wear resistance
- To improve fatigue life
- To improve corrosion resistance (except for stainless steels)
- To obtain a surface that is resistant to the softening effect of heat at temperatures up to the nitriding temperature

#### **2.4.1 Previous Studies on High Temperature Gas Nitriding (HTGN)**

As the author have mentioned earlier, the process method of nitriding that the author will conduct is the gas nitriding at high temperature (HTGN) method. According to C.M. Garzon, A.P. Tschiptschin, in this high temperature gas nitriding (HTGN), atomic nitrogen is absorbed at the surface of the steel and then diffuses into the near surface region [21]. Furthermore, he also stated that the high treatment temperature ( $\sim 1400\text{K}$ ) allows dissolving high nitrogen contents ( $\sim 0.5\text{-}1.0\text{wt. \%}$ ) in the austenitic range without inducing nitride formation. He also have made a comparison between this treatment with conventional gas nitriding (low temperature gas nitriding) as discussed before which usually performed between  $750\text{K}$  and  $850\text{K}$  which showed quite different condition where intense chromium nitride precipitation occurs, and greatly increasing the hardness but impairing the corrosion resistance of stainless steel nitrided parts [21].

On top of that, the author also have take consideration of other types of stainless steel such as austenitic stainless steel and according to Nakanishi (2007), he stated that an attempting to improve the mechanical properties and corrosion resistance of commercial 316L austenitic stainless steel plates by means of “solution nitriding” (nitrogen absorption treatment or high temperature gas nitriding (HTGN) [11], which is one of chemical heat treatments to add nitrogen into stainless steel. It is

well known that the nitrogen addition to austenitic stainless steel has many advantages including:

1. The tensile strength of the steels drastically increase without reducing the ductility too much
2. The transformation to martensitic structure (generation of magnetism) can be reduced
3. Corrosion resistance, especially pitting corrosion resistance is improved
4. Nitrogen is considered to be harmless to the human body

Solution nitriding is a simple and powerful technique to obtain high nitrogen stainless steel without requiring any special equipment [11, 20].

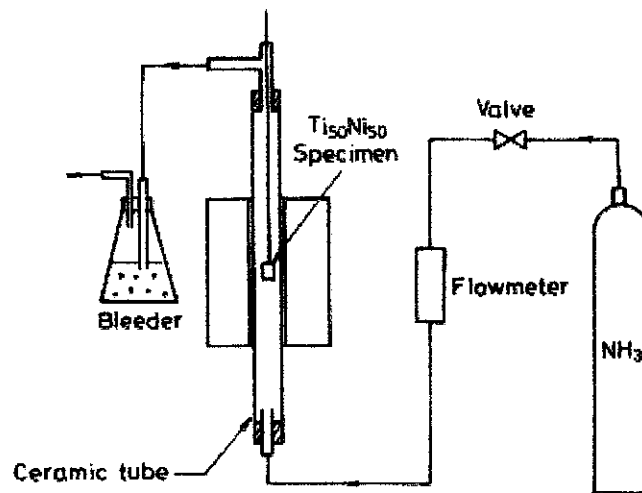


Figure 5: Schematic illustration of the gas nitriding equipment [11]

A new high temperature gas nitriding (HTGN) treatment that allows obtaining high nitrogen cases, about 1 mm in depth, on stainless steels was developed. Jose Francisco and Carlos Mario showed that when HTGN is applied to austenitic–ferritic, martensitic and austenitic stainless steels, their cavitation erosion (CE) resistance is considerably increased [12]. Additionally, quite different from conventional gas nitriding, where ammonia–hydrogen (NH<sub>3</sub>–H<sub>2</sub>) gas mixtures are used, the HTGN treatment is performed in still (N<sub>2</sub>) gas atmosphere which is neither explosive nor toxic. As gas flux and gas control equipments are not necessary, energy losses and costs are diminished [12].



Referring to K.Y.Li and Z.D.Xiang (2010), the growth rate of the nitrided layer can be increased by increasing the nitriding temperature, which is the basis for development of the solution nitriding or high temperature gas nitriding process for stainless steel [13]. The process is carried out at temperatures above 1050°C in pure nitrogen normally only for few hours and a hardened case layer over 300µm can be provided with a gradual nitrogen concentration, and hence hardness, profile from surface to inner parts of the substrate. Because the nitrogen solubility in the  $\gamma$ -phase decreases at higher nitriding temperatures, nitrogen pressure higher than normal atmospheric pressure is often used in the nitriding process to compensate for the decreased nitrogen solubility [13].

Furthermore, not only the nitrided layer can be increased, but there is a significance regarding the changes of microstructure after been nitrided. This is due to, according to the research that had been done by Department of Materials Science and Engineering, Dong-A University, HTGN was introduced as a method for adding nitrogen into stainless steels which involve a diffusion process for nitrogen, a strong austenitic forming element [16]. The research paper mentioned that the purpose is to permeate the surface stainless steel through heat treatment in N<sub>2</sub> atmosphere at high temperatures. When nitrogen permeates from the surface into the interior of stainless steel, the surface microstructure changes into austenite or martensite, depends on the amount of nitrogen permeated and the process temperature [16, 21]. As a result, the hardness of the surface layers increase.

In term of microstructure changes, according to Hans Berns in his paper with titled, *"Reduction in wear of sewage pump through solution nitriding"*, the specimens that he used was centrifugal pumps [22], with impellers and discs made of a stainless duplex steel which in line with the sample material that the author used. He stated that the microstructure of the solution nitrided samples undergoing few changes. The figure below shows the microstructure of the nitrided duplex stainless steel.

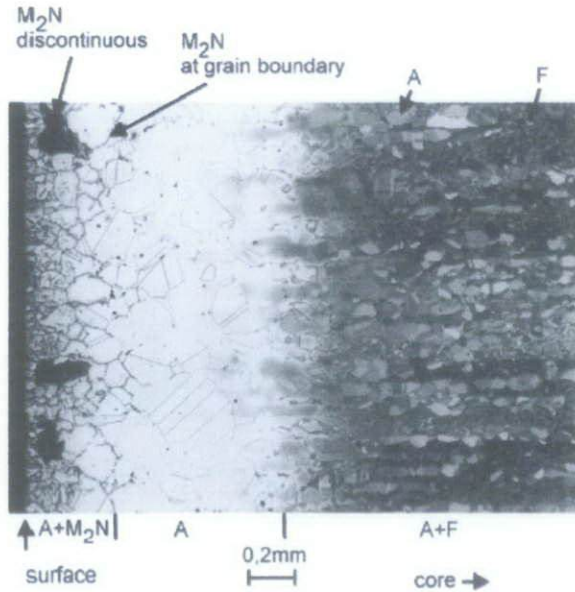


Figure 6: Section through the solution nitrided case of the duplex stainless steel. The microstructural constituents are: austenite (A), ferrite (F), nitride ( $M_2N$ ) [22]

From the microstructure image above, at the left which is at the surface, the content of ferrite is reduced by increase of nitrogen. The precipitation of  $M_2N$  is observed along the grain boundaries and in lamellar form within some grains. According to him, this discontinuous morphology is called ‘nitrogen pearlite’ and the nitride lamellae are also remains austenitic [23]. According to P.Hussain on his paper titled, “*Formation of Nitrogen-Pearlite in the Diffusion Bonding of Sialon to 316L Stainless Steel*”, it has concluded that the  $M_2N$  precipitation is in the form of  $Cr_2N$  has been precipitated at the grain boundary, by discontinuous precipitation (cellular phase transformation) and finally, intragranular within the matrix [24]. This could be guidance for the author to explain if the same precipitations occurred in her experiments.

The researchers from Dong-A University also believed that HTGN of the ferritic AISI 430 stainless steels enable the nitrogen to permeate into interior due to relatively low carbon and high Cr content and a martensite structure is formed [16]. Not only will that, with conducting the gas nitriding at high temperature, nitrogen will diffuse interstitially which is in between the atom or the crystalline structure of the atom or in the other word, it will form the solid solution in the crystal structure [6, 16]. Therefore the hardness surface of the sample will be increase due to that

condition. Figure 7 below shows the hardness variation with depth below the surface after the HTGN treatment for this steel [16].

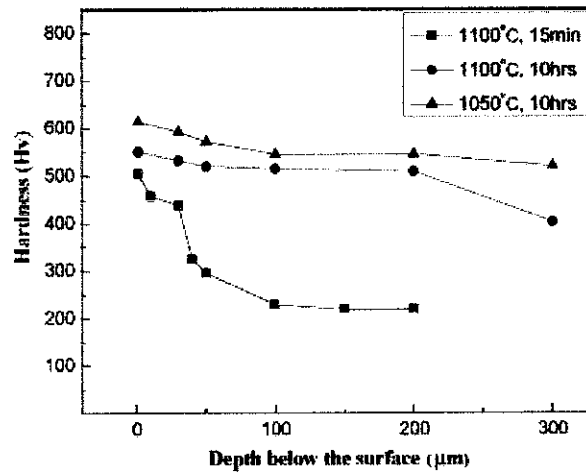


Figure 7: Hardness as a function of the depth below the surface after HTGN treatment for 10 hr [16]

The trend from the figure above is that the hardness decreased gradually in proportional to the nitrogen content at 1100°C for 15 min. However, the hardness was relatively unchanged until 200μm from the surface (~500Hv) at 1100°C for 10 hr. Moreover, the highest hardness (~600Hv) was observed at 1050°C for 10 hr. This hardness variation is related to the nitrogen content and phases appeared on the surface layers. At 1050°C, the precipitation of  $\text{Cr}_2\text{N}$  might increase the hardness. Yoo et al [17] reported that these effects of the precipitation of nitrides have an influence on the increase in the hardness of the surface. Folkhard [18] also reported that nitrogen introduces strong elastic distortions into the crystal lattice and increases the internal friction, thus making the movement of dislocations through the lattice more difficult. For this reason, the nitrogen solid solution strengthening at the surface promotes the increase in hardness afforded by the precipitates [10].

On top of that, from the discovery by C.M. Garzon [23] in this journal named, *EBSD texture analysis of high temperature gas nitride duplex stainless steel*, he had stated that in this HTGN treatment, atomic nitrogen is absorbed at the steel's surface from a  $\text{N}_2$  gas atmosphere, and then diffused into the core direction. The high temperature treatment allows dissolving high nitrogen contents (~0.15-1.0wt %) in the austenitic range without inducing nitride formation. Not only that, he also mentioned that

lower nitriding temperature inducing  $M_2N$  nitride precipitation at the austenitic surface layer and higher nitriding temperature leading to excessive fraction of ferrite in the non-nitride core [9, 23].

On the other hand, according to the research made by E.Erisir [8] on his paper in title “*Effect of precipitation on hot formability of high nitrogen steels*”, he carried out the experiments for three types of stainless steel grades of 1.4501, 1.4882, and 1.4452 of high nitrogen steel and austenitic grade 1.4301 steel. From his discovery, he investigated the precipitation characteristics and phase transformation by calculation of phase diagrams and precipitation analysis using SEM/EDX [8]. As the author will conduct the HTGN process for duplex stainless steel, it is an important step for the author to understand the phase diagram of duplex stainless steel and for this case using 1.4501 grade of stainless steel which involves the precipitation that might occur upon the heat treatment with nitrogen flow in it. The figure below showed the phase diagram of 1.4501 in the function of nitrogen content.

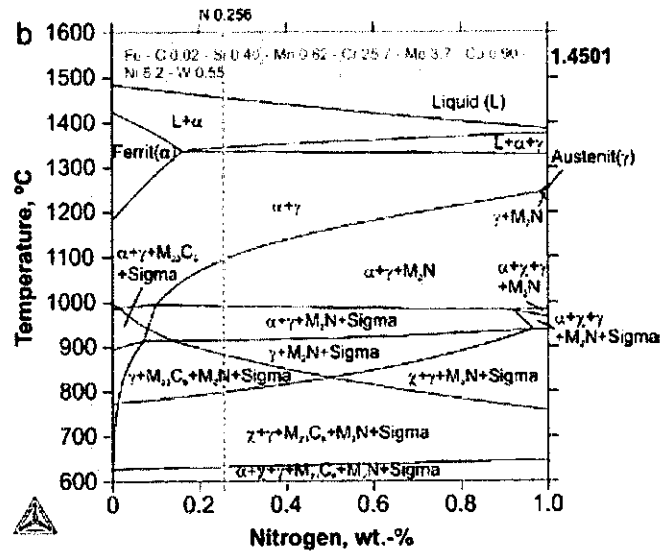


Figure 8: Phase diagram of grade 1.4501 versus nitrogen content [8]

This figure was calculated using the Therm-Calc software in order to predict the stability of occurred phases and precipitates. Figure 8 is an isopleth diagram showing stability of phases as a function of temperature and nitrogen content. The dashed line in this diagram indicates the relevant nitrogen amount for steel compositions used here [8]. This figure also explained that the possibility of nitrides in the form of  $M_2N$  phases can also precipitate as the temperature starts cooling down from the range of

1100°C-1300°C. Intermetallic sigma and chi ( $\chi$ ) phases also could precipitates. Typical deformation temperatures lies between 900°C and 1300°C for investigated steel and nitrides may exist within the temperature deformation and  $M_2N$  are stable for this grades of duplex stainless steel. This figure could be a guidance for the author in order to predict the phases that might precipitates as the samples will undergoing high temperature nitriding and will have a significant amount of nitrogen diffused into the steel [8].

On the other hand, the author also took a reference from other type of nitriding process such as low temperature active screen plasma nitriding. From Kimiaki Nagatsuka [7] with his journal titled, “*Surface hardening of duplex stainless steel by low temperature active screen plasma nitriding*”, stated that plasma nitriding carried out below 723K forms a nitrided layer that is called S phase. This phase improves the surface hardness without decreasing the corrosion resistance. The nitrided samples were analyzed by carrying out various tests. One of the tests is X-ray diffraction measurement [7]. The result is shown as per below.

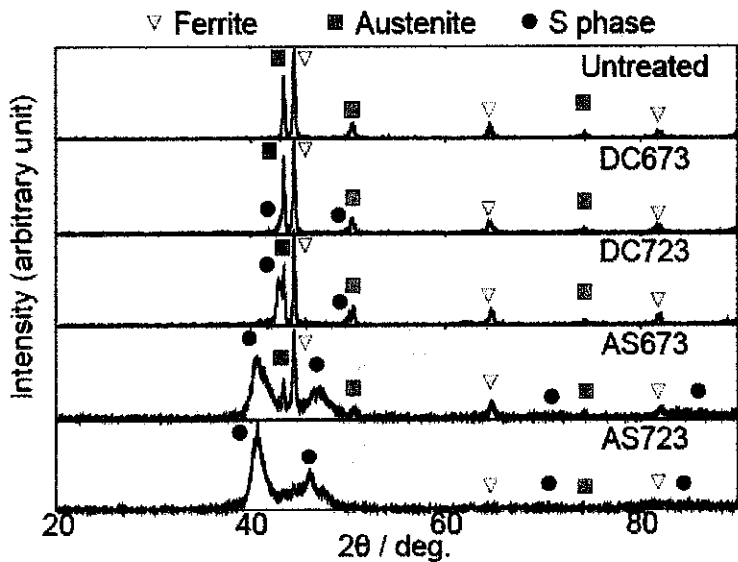


Figure 9: X-ray diffraction result of plasma nitrided of duplex stainless steel [7]

As been shown in the figure above, the untreated sample showed an assorted structure of ferrite and austenite. The surface of the nitrided samples consists of ferrite, austenite, and an S phase [7]. The S phase is considered to be a supersaturated solid solution of nitrogen in an austenitic phase. The author will consider and take note the pattern of the XRD result for untreated sample of duplex

stainless steel and will bear in mind if the S phase will might also appear in the microstructure after all her samples have undergoing nitriding process and the results have been discussed in chapter four.

From all the discoveries from numbers of journals that the author has come across, it shows that there are significance effects of variations of nitriding temperature towards the other types of stainless steel samples and also duplex stainless steel in term of surface hardness, growth rate of nitrided layer and microstructure changes. Therefore, in order to prove all the statements mentioned by numbers of the researchers previously, the author have conducted the HTGN process with using duplex stainless steels at four different temperatures namely at 1100°C, 1050°C, 1000°C and 950°C at constant time of six hours and compared all the results for the use in future work since there is no research or paper work that using this kind of material which undergoing high temperature gas nitriding (HTGN) with variations of temperatures used yet. Indeed, it has been reported that titanium alloys can be nitrided under a low nitrogen pressure of decomposition of  $\text{Cr}_2\text{N}$  powder without causing the formation of titanium nitrides. This finding may be of significance with relevance to nitriding of stainless steels as it is more difficult to suppress the formation of titanium nitrides than the formation of chromium nitrides, although the solubility of nitrogen is higher in titanium alloys than in stainless steel [9, 10].

## CHAPTER 3: METHODOLOGY

### 3.1: Project Flow Chart

Initially, the author had read some journals and articles for the literature review in order to enhance the understanding on mechanical properties, microstructure changes and hardness profile for nitrided samples. This chapter describes the procedures and methods involved in completing the experiment. This is including the procedure in conducting or managing the fluidized bed furnace. Besides, the optical microstructure test, X-ray diffraction analysis and hardness test procedure are discussed here. All stages are illustrated in the research methodology flowchart. Below shows the several steps which will accomplish by the author for this project:

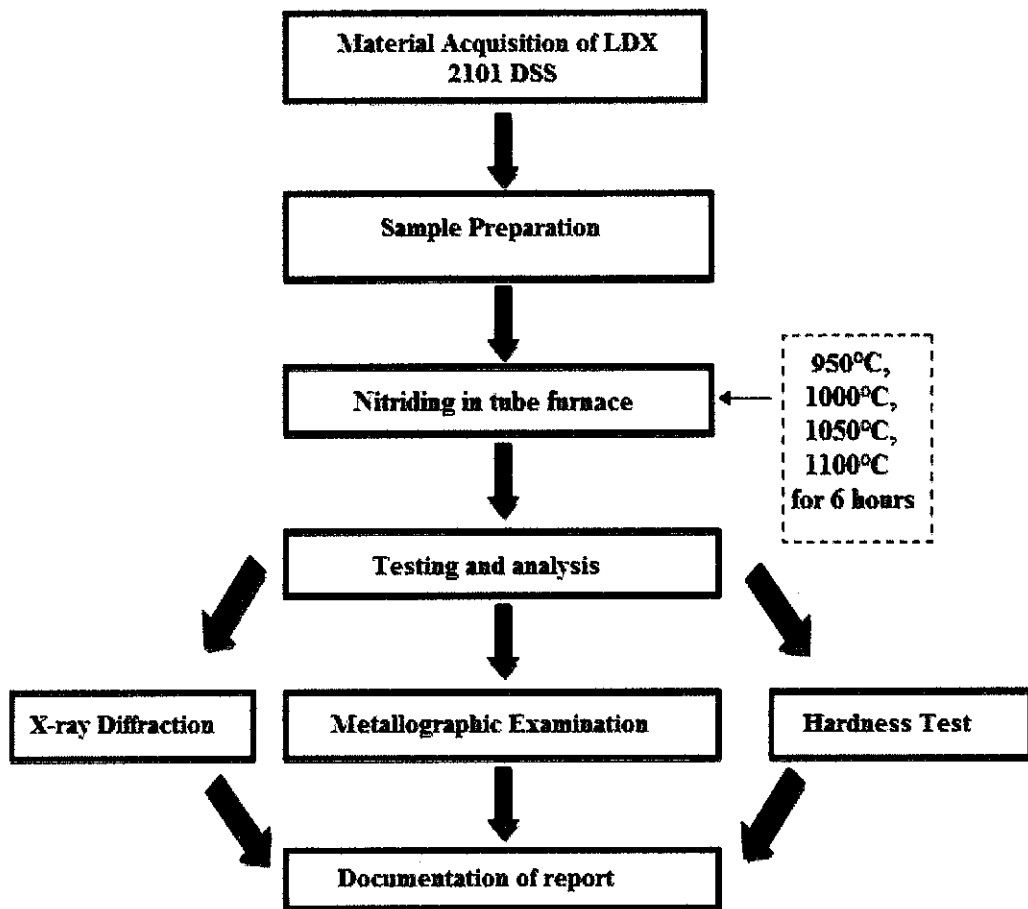


Figure 10: Project's flow chart

### **3.2 Procedures**

In completing this project, there are few steps and procedures will be taken to ensure that the objectives of the project are fulfilled.

#### **3.2.1 Research Methodology**

- Identifying real problem and project objectives
- Revision of the crystal structure and phase (LDX 2101 of duplex stainless steels)
- Get familiar with stainless steel (specially LDX 2101 of D.S.S ) and the types in industry
- Find a suitable method that will be used in analyzing the brittleness
- Survey any related info and literature review using journals, books, magazine and internet

#### **3.2.2 Material Acquisition**

The material used in this project is LDX 2101 stainless steel. The material was chosen because it is widely used as pipeline in oil and gas industry. Besides that, nitriding has potential to increase the surface properties of this duplex stainless steel. Nitrided duplex stainless steel will have good properties compare to the untreated one thus can increase its performance in industry application.

#### **3.2.3 Sample Preparation**

The material obtained by the author at the first time is in the plate pattern and need to be cut in order to prepare for this project. The materials need to be cut to rectangular shape 15mm X 10mm X 5mm. After cutting the first sample, the sample was prepared for analysis of as received sample which then will be recorded to compare with the nitrided samples.

##### Step 1: Cutting of specimen

A plate of duplex stainless steel was cut into numbers of pieces. All the samples have been undergoing cutting process with using the wire cut machine or Electrical Discharge Machine (EDM) which located at block 16 as shown in Figure 11 below. The author choose to used EDM as a cutting machine to make a specimen because the *Electrical discharge machining (EDM) is a machining method primarily used for hard metals or those that would be very difficult to machine with traditional*



techniques. The sample size that needs to be cut must be around 10mm to 20mm for convenience during grinding and polishing. Twelve specimens were prepared for this project. The size of the sample after cutting is around 15mm X 10mm X 5mm.



Figure 11: Electrical Discharge Machine (EDM)

### Step 2: Grinding

The specimen was ground using grinder shown in Figure 12 below. It was ground on progressively finer SiC waterproof papers from 120 to 1200 grit, to produce a reasonably flat surface; it is lubricated with water to keep it cool and to remove the grinding products. If the sample is not flat, it might be necessary to remove some material on the lathe or grinding machine first. The sample should be moved forward and backward on the paper until the whole surface is covered with unidirectional scratches. It is then washed with running water to remove debris associated with the grade of paper used. It is then ground on the next finer paper such that the scratches produced are at right angles to those formed by the previous paper.



Figure 12: Grinding Process

### Step 3: Polishing

Due to the very small depth of field obtained from an optical microscope it is essential that the surface is flat, in fact it needs to be optically flat, acting as a perfect mirror. The specimen therefore has to be “polished”. This is done using rotating wheels covered with a cloth impregnated with a very fine abrasive compound. The compounds used are diamond. The 1  $\mu\text{m}$  diamond wheel is used. The specimen is pressed down onto the lubricated rotating wheel. It is important not to hold the specimen in one orientation for an extended time as it will cause “dragging” of some microstructural components. After 20-30 seconds the specimen is removed and rotated through 90° in the hand, placed back on the wheel and then again oscillated. This process is continued until the fine scratches have been removed.

### **3.2.4 Nitriding Process**

The nitriding process was done in a Lenton horizontal tube furnace as shown in Figure 13. It is located at Block 17. The nitriding temperature was 950°C, 1000°C, 1050°C and 1100°C. The nitriding time for all temperature was six hours. As in the furnace room is completed with the oxygen indicator, the purpose is to identify the percentage of nitrogen gas that been used up for the nitriding process. The author will wait until the percentage of oxygen is low enough as indicating the nitrogen gas has been fully flowing to the tube furnace, and then the author will start the experiment. The total gas flow rate was 1000cm<sup>3</sup>/min. The flow rate was control using a flow meter as shown in Figure 14. Before starting the nitriding procedure, the furnace needs to be arranged properly. The samples must be cleaned using

ultrasonic cleaner before putted inside the furnace. The weights of the samples were measured before and after nitriding.



Figure 13: Lenton Horizontal tube furnace



Figure 14: Flow meter

#### Step 1: Furnace arrangement

The furnace needs to be connected with nitrogen gas. The exhaust of the furnace must be connected with fume hood for safety reasons. As the author had mentioned before about the oxygen indicator that functioned to indicated the percentage of presence oxygen gas in the tube furnace. This is because, before starting the nitriding process, the author need to ensure that there was low enough oxygen gas to avoid the oxidation that will interrupt the nitriding process. Not only have that, the scrubber coned flask also connected to the tube furnace before the gas tube connected to the fume hood. The scrubber cone flasks will be function to avoid the water or nitrogen gas flowing back to the furnace. The figure below shows the oxygen indicator and the scrubber cone flasks.



Figure 15: Oxygen indicator



Figure 16: Scrubber cone flask

#### Step 2: Ultrasonic cleaning

Before putting the samples inside the furnace, it must be cleaned using ultrasonic cleaner. The purpose of this cleaning is to remove any debris that contain at the sample's surface. The samples were immersed with acetone inside a beaker. Then, the beaker was putted inside an ultrasonic cleaner. The cleaning time was 10 minutes. The ultrasonic cleaner can be seen in Figure 17.



Figure 17: Ultrasonic cleaner



### Step 3: Nitriding

After cleaning the samples, the samples were putted in alumina boat. The alumina boat can be seen in Figure 18. The alumina boat will be placed at the center of the furnace. Steel wire was used to push the alumina boat to the center of the furnace. The furnace needs to be purged using nitrogen gas for until the oxygen indicator shows the lowest percentage of oxygen gas in order to remove the oxygen gas and any gas inside the furnace from previous experiments. After purging, the furnace will be heated. The heating rate was 15°C/min. During heating, nitrogen gas still flowing in the furnace until the temperature reached the nitriding temperature (950°C, 1000°C, 1050°C and 1100°C). The nitriding holding time was 6 hours for each temperature. The samples were furnace cool until the temperature down to the room temperature.

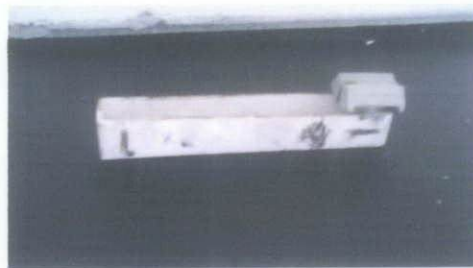


Figure 18: Alumina boat

### **3.3 X-ray Diffraction Analysis**

Generally, X-ray Diffraction is used to characterize the crystallographic structure and the technique that is commonly used is power method. In this technique a powdered specimen is utilized so that there will be a random orientation of many crystals to ensure that some of the particles will be oriented in the x-ray beam. It is also equipped with x-ray diffractometer that has a radiation counter to detect the angle and intensity of the diffracted beam [14]. A recorder automatically plots the intensity of the diffracted beam as the counter moves on a goniometer cycle that is in synchronization with the specimen over a range of  $2\theta$  values. Commonly, the diffraction angles and intensities are plot simultaneously.

Since the wavelength of some x-rays are about equal to the distance between planes of atoms in crystalline solids, reinforced diffraction peaks of radiation of varying

intensities can be produced when a beam of X-rays strikes a crystalline solid. A monochromatic beam of X-rays are to be incident on a crystal. If the reflected wave patterns of the beam leaving the various planes are in phase, then reinforce of the beam or constructive interference occurs as shown in Figure 19.

Consider the incident x-rays 1 and 2 as indicated in Figure 19. For these rays, the extra distance of travel of ray 2 is equal to  $MP + PN$ , which must be an integral number of wavelength  $\lambda$ . Thus,

$n\lambda = MP + PN$  where  $n = 1, 2, 3, \dots$  and is called the order of the diffraction.

Since both  $MP$  and  $PN$  equal  $d \sin \theta$  where  $d$  is the interplanar spacing of the crystal planes of indices  $(hkl)$ , the condition for constructive interference must be:

$$n\lambda = 2 d \sin \theta$$

The equation is known as Bragg's law and in most cases, the first order of diffraction where  $n=1$  is used. Therefore, Bragg's law takes the form

$$\lambda = 2 d \sin \theta$$

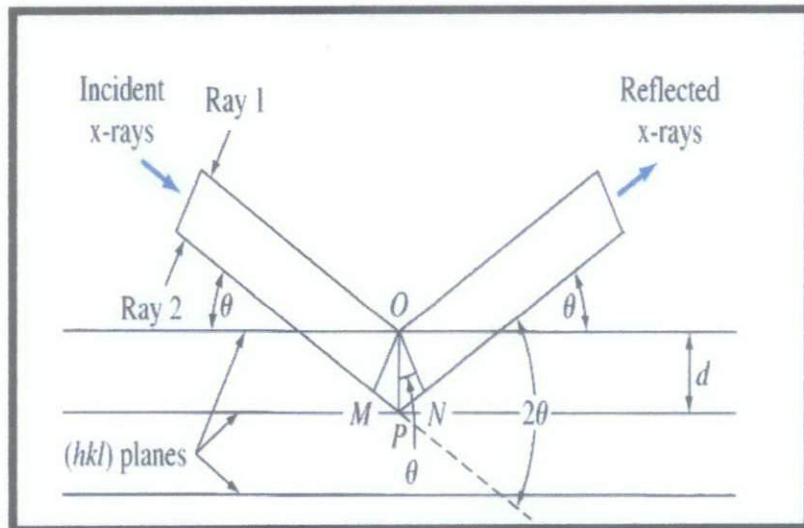


Figure 19: The reflection of an X-ray beam by the  $(hkl)$  planes of a crystal [14]

In the present investigation of nitriding of carbon steel, the purpose of X-ray diffraction analysis is to determine the formation of alloying nitride subsequent to nitriding process. This will indicate the effectiveness of the process in collaboration

with the hardness test and micrograph examination. The x-ray Diffraction machine used for this investigation was located at Block 17 as shown in Figure 20.



Figure 20: X-ray Diffraction Machine [14]

**3.4 Microstructure Examination**

The purpose of this test is to examine the formation of nitride layer subsequent to nitriding process. This test was conducted using optical microscope and scanning electron microscope. The chemical composition of the samples can be determined using energy-dispersive X-ray spectroscopy that being attached together with the scanning electron microscope [15]. The optical microscope is located at Block 17 as shown in Figure 21 while the scanning electron microscope is located at Block P as shown in Figure 22.

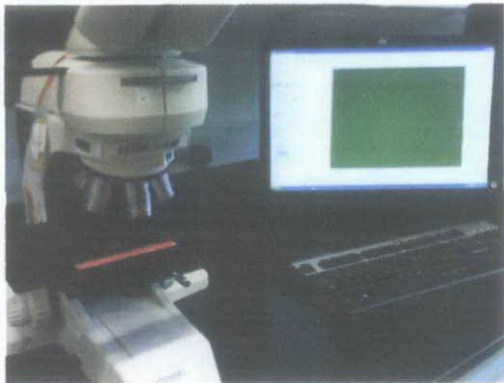


Figure 21: Microstructure examination using optical microscope



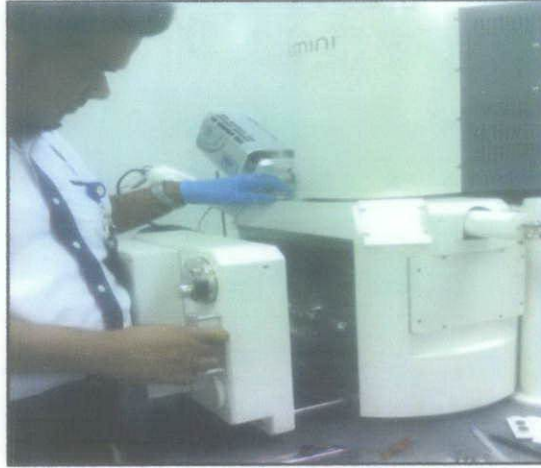


Figure 22: Scanning electron microscope

In addition, after nitriding, the nitrated samples need to be cut into two parts. One part was used for the metallographic and microstructure analysis using optical microscope (OM) and scanning electron microscopy with energy dispersive x-ray spectroscopy (SEM-EDX) and lastly for the hardness measurement. The other part was used for the X-ray diffraction analysis (XRD). Before conducting the microstructure examination, the samples need to be mounted, grinded, polished and etched. Mounting of specimen is required so that it is more convenient during grinding and polishing. Specimen was mounted in a resin. Bakelite is commonly used. A further advantage of mounting is that the edges of the specimen will be reasonably well polished and not “bevelled” by the preparation process.

After mounting, the samples need to be grinded and polished. The method for this procedure has been discussed earlier.

For duplex stainless steel, the etchant used is fry reagent. The purpose of etching is to reveal the grain boundary. Firstly, the specimen was washed using ethanol and then dried. After that, fry reagent was applied at the surface of the specimen for 5 to 10 seconds. Then the specimen was washed using water and alcohol. The specimen was dried and ready for microstructure examination. The figures below showed the image of fry reagent, samples that been etched, ethanol, and dryer.



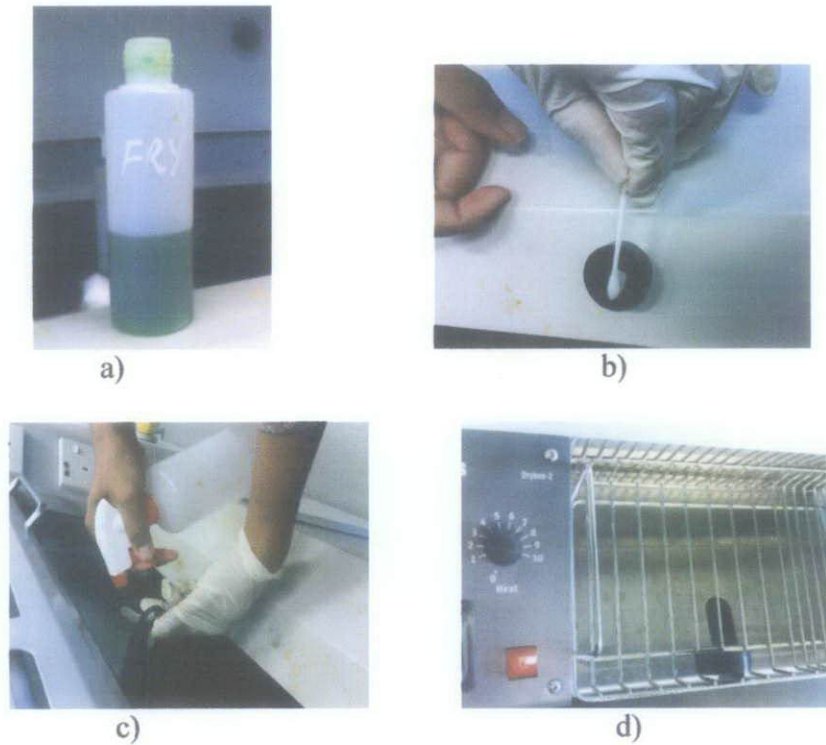


Figure 23: a) Fry reagent, b) Applying etching solution, c) Applying ethanol, d) Drying the sample using heat dryer

### 3.5 Hardness Test

The hardness test was carried out by pressing a ball or a point with a predetermined force into the surface of the specimen. Three most commonly used methods are Brinell, Vickers and Rockwell hardness test. The measuring location on the specimens must have a bright, polished surface to prevent erroneous measurements due to rough grooves.

In this investigation, the method used for the hardness measurement is Vicker Hardness test as shown in Figure 24. Hardness is the measurement of material surface resistance to indentation from other material by static load. Indentation body is a square based diamond pyramid with 136 included angles. The average diagonal (d) from the adjustable shutters of the impression is converted to a hardness number [19]. The indented image will be displayed in the calibrated Microscope screen [19]. The load used for this test was 25 gf. The dwell time was 15 second.

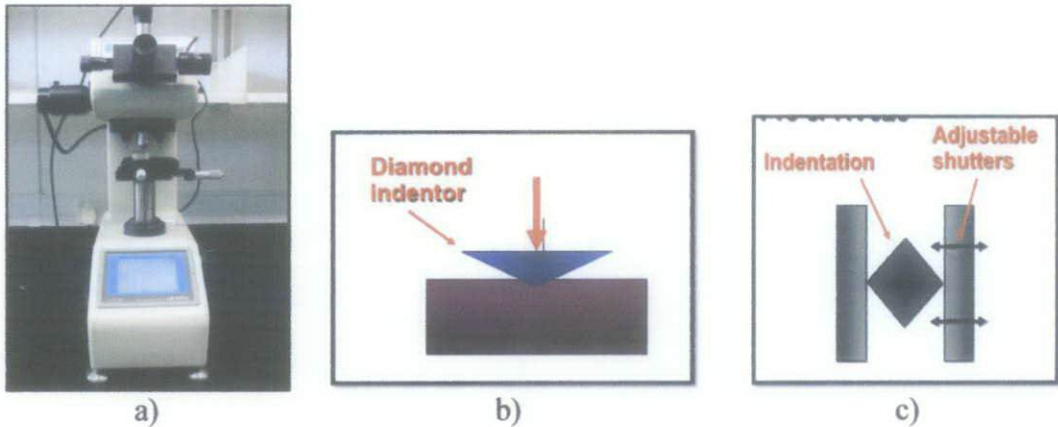


Figure 24: a) Vickers Hardness Equipment

b) Diamond Pyramid Indentor

c) Adjustable Shutters

### 3.5.1 Vickers Test Method

Vickers indenter All Vickers ranges use a  $136^\circ$  pyramidal diamond indenter that forms a square indent. The steps are [19]:

- i. The indenter is pressed into the sample by an accurately controlled test force
- ii. The force is maintained for a specific dwell time, normally 10-15 seconds
- iii. After the dwell time is complete, the indenter is removed leaving an indent in the sample that appears square shaped on the surface
- iv. The size of the indent is determined optically by measuring the two diagonals of the square indent.
- v. The Vickers hardness number is a function of the test force divided by the surface area of the indent.

3.6 Gantt Chart

Table 2 and table 3 below is Gantt chart showing the timeline allocated by the author for FYP I and FYP II in order to complete the project.

Table 2: The milestones of FYP 1 project research

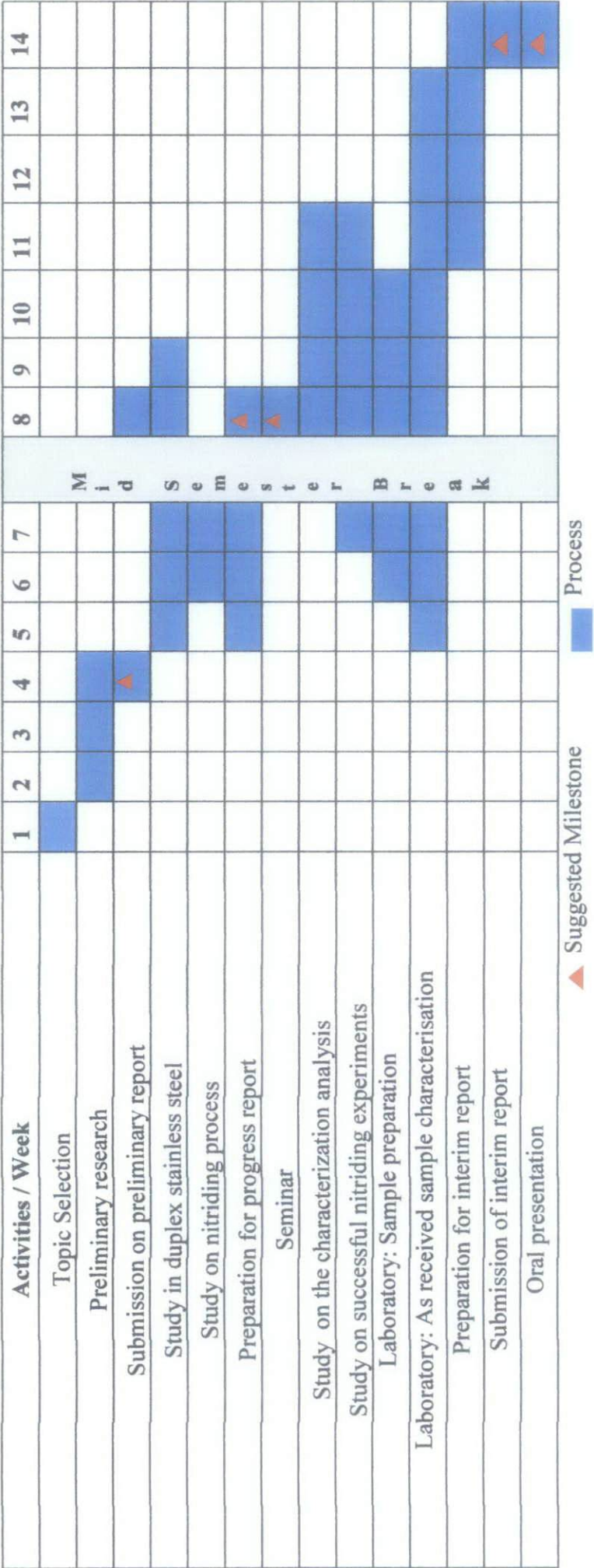


Table 3: The milestone of FYP II project research

Activities / Week	1	2	3	4	5	6	7	M i d S e m e s t e r B r e a k							12	13	14
Arranging furnace																	
Nitriding process																	
Metallography characterisation																	
XRD characterisation																	
Submission of progress report																	
Surface hardness testing																	
Pre-EDX																	
Submission of draft report																	
Submission of dissertation (softbound)																	
Submission of technical paper																	
Oral presentation																	
Submission of dissertation (hardbound)																	

▲ Suggested Milestone      ■ Process



## CHAPTER 4: RESULT AND DISCUSSION

### 4.1 Introduction

This chapter offers the experimental results of the untreated (as received) and heat treated of duplex stainless steel through nitriding process. The parameters were variation of temperatures of the nitriding process. The results were obtained from the weight measurement analysis, hardness test, microstructure analysis and x-ray diffraction analysis. The experiments were carried out in 950°C, 1000°C, 1050 °C and 1100°C for constant time of six hours. The processing parameters were compared with respect to nitriding temperature.

After nitriding which has been carried out in Lenton Horizontal Tube Furnace, various techniques were used to characterize the structure, composition, hardness and phases of the unnitrided and nitrided samples. The analyses of structure and composition included visual examination, the theta-2theta X-ray diffraction (XRD) analysis for identification of nitride phases, and field emission scanning electron microscopy (FESEM), optical microscope (OM) and energy dispersive X-ray spectroscopy (EDX). The hardness test was performed using a Vickers microhardness tester under 25 gf load. All these result were analysed and compared between the unnitrided and nitrided samples so that the author would emerge with a new founding towards this type of material which is duplex stainless steel undergoing high temperature gas nitriding treatment.

### 4.2 Mass/weight differences before and after nitriding

Nitriding will cause diffusion of nitrogen into the metal. The diffusion can increase the weight of the samples. If the weight of the samples increases after nitriding, it shows that nitrogen diffusion at the surface occurred. Table 4 below shows the weight of the samples before and after nitriding process for 950°C, 1000°C, 1050°C and 1100°C. From Figure 25, the graph shows that the percentage of weight difference of samples before and after nitrided increase gradually with temperatures. It can be concluded that, the nitrogen diffusion increases when the nitriding temperatures also increases.

Table 4: Weight of samples on particular nitriding temperatures

Nitriding Temperature °C	Mass before (g)	Mass after (g)	Weight Difference (g)	Percentage of weight different (%)
950	7.322	7.327	0.005	0.068
1000	7.418	7.426	0.008	0.108
1050	7.387	7.397	0.010	0.135
1100	7.474	7.492	0.018	0.240

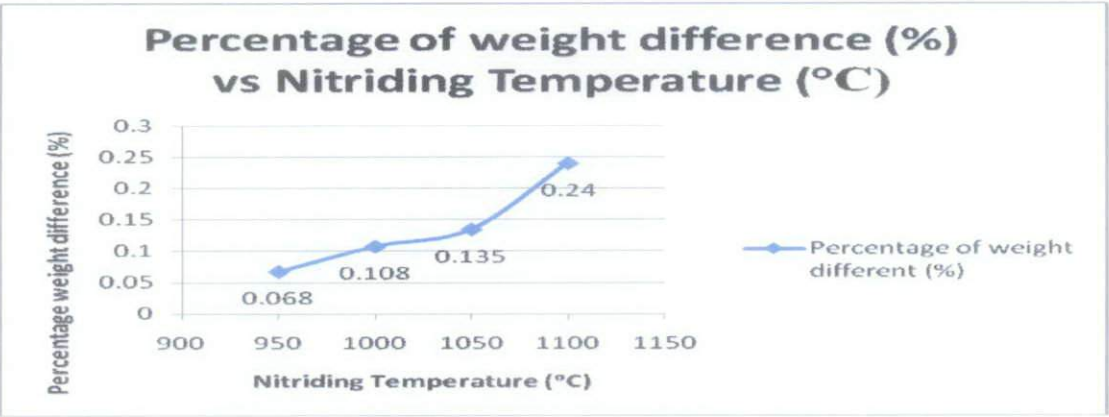


Figure 25: Percentage weight difference vs Nitriding temperature for unnitrided sample and nitrided samples

4.3 Vickers Microhardness

The Vickers (HV) test was developed in England in 1925 and was formally known as the Diamond Pyramid Hardness (DPH) test. The Vickers test has two distinct force ranges, micro (10gf to 1000gf) and macro (1kgf to 100kgf), to cover all testing requirements.

Hardness test was conducted to determine the characteristic of each specimen under the influence of the processing parameters such as nitriding temperatures. Microhardness Vickers test were conducted to the specimens from the distance of the bakelite or mounting which is from the outer surface of the samples. The load used was 25 gf and the dwell time was 15 second. Therefore, the result is shown in Table 5 and the trend of the hardness profile of these samples is provided in Figure 26 as per below.

Table 5: Microhardness data of unnitrided sample and nitrided samples

Distance (μm)	Vickers Microhardness (HV)				
	Unnitrided	950°C	1000°C	1050°C	1100°C
0	234.3	318.2	385.6	408.0	448.2
50	227.6	281.0	328.7	366.7	428.6
100	231.5	257.4	291.4	331.8	411.8
150	228.2	246.3	265.9	293.4	405.3
200	219.3	245.7	259.2	272.9	398.2
250	226.8	245.4	258.2	258.8	393.8
300	214.9	244.8	252.1	257.5	387.4

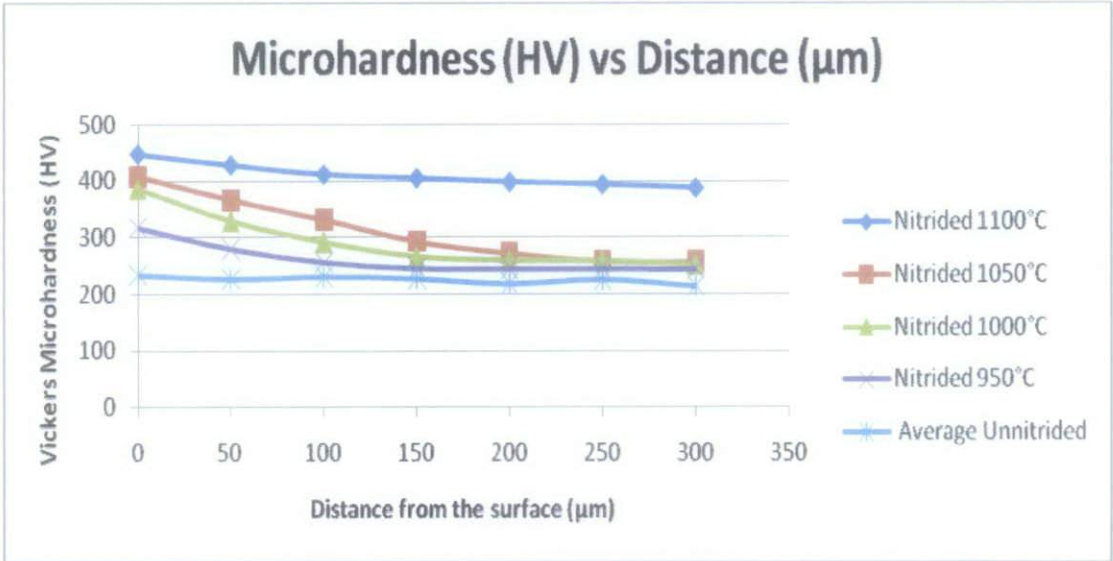


Figure 26: Hardness profile over distance from the surface to the minimum distance of the core of the steels

From the figure above, the microhardness profiles of the cross section of the nitride surface shows the effectiveness of the treatments to increase the surface hardness of the steel was verified. It was seen that the nitriding temperature influences the hardness of the surfaces. The nitride surface obtained at 1100°C had a higher microhardness value due to the presence of chromium nitrides and iron nitrides at the surface phases and the same as the other surfaces at the other three samples. This can attribute to the temperature dependence of the dispersion hardening of the nitride

precipitate within the matrix. Higher treatment temperatures results in precipitate coarsening of the matrix. Precipitates which in this case, nitrides with particular size and density will be the most effective in preventing the movement of dislocations and in achieving the highest strengthening and hardness of the samples mostly at the outmost surface. It can be seen that the effect of nitriding temperature on hardening behaviour is displayed in term of the case depth (distance from surface) which is governed by the extend of nitrogen atoms penetration into the samples surface, thus increases for increasing temperatures due to increased nitrogen diffusion coefficient. This increase in hardness can be due to the lattice distortion caused by nitrogen atoms at interstitial sites in supersaturated Fe-N solid solution and the precipitation of coarse grained nitrides.

Not to forget, the pattern of the hardness profile that the author obtained shows that the hardness value decreases as the distance move farther from surface. However, the hardness was relatively changed until to 200 $\mu$ m and relatively unchanged or constant for the distance farther than that. This can be concluded that the nitrogen diffusion and the formation of nitrides which resulted in significant hardening the metal just only occurred at the surface of the samples. The behaviour of the nitride precipitates will be discussed further later in the next part.

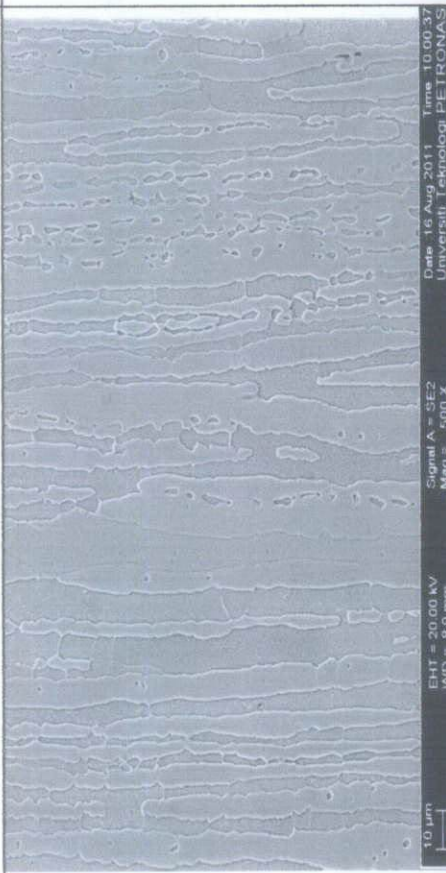
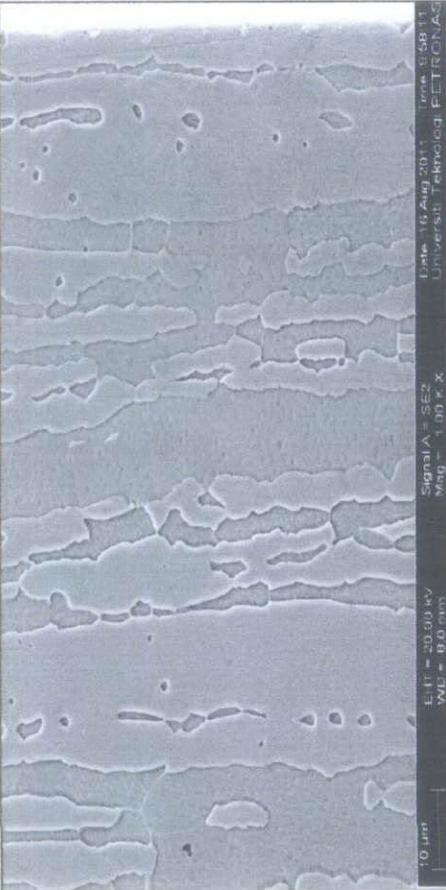
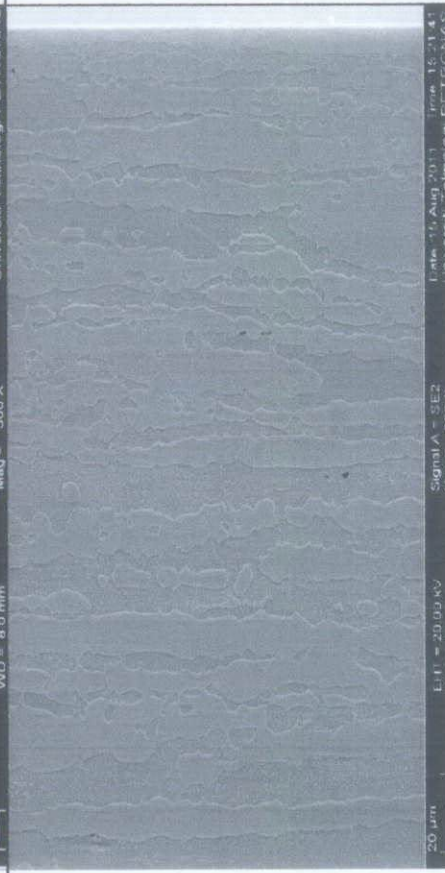
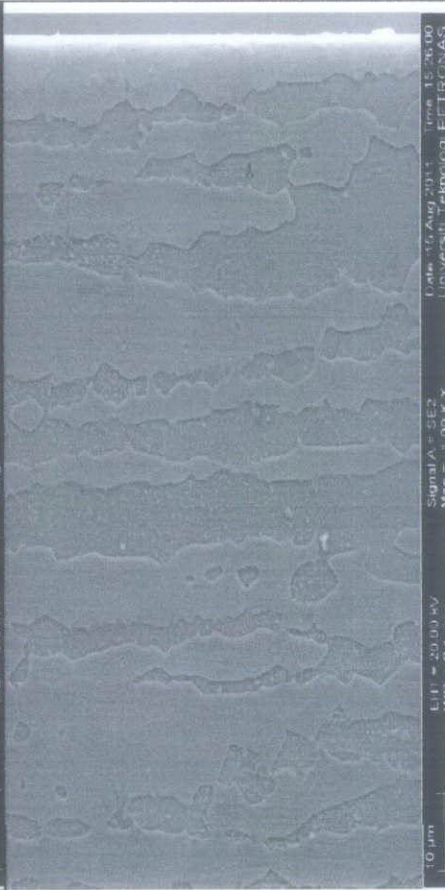
#### **4.4 Microstructure and morphology Analysis**

The microstructures of four nitrided samples of duplex stainless steel were analyzed using FESEM at magnification of 500X and 1000X. From the result, Figure 27 below shows the microstructure images of the samples of duplex stainless steel at of unnitrided and four different temperatures and there were significant variation in term of the surface phase changes at the microstructures.

Furthermore, the author also observed the microstructures of the unnitrided sample and the other four nitride samples by using optical microscope (OM). The microstructures of all the samples were observed and analyzed at magnification 100X.



4.4.1 SEM – Microstructure Images on surface layer

Sample	Magnification 500X	Magnification 1000X
Unnitride d (As received sample)		
Nitrided at 950°C		

<p>Nitrided at 1000°C</p>	 <p>10 µm</p> <p>UHV = 20.00 kV WD = 8.0 mm</p> <p>Signal A - SE2 Mag = 1.00 K X</p> <p>Date: 15 Aug 2011 Time: 16:00:27 Universiti Teknologi PETRONAS</p>
<p>Nitrided at 1050°C</p>	 <p>10 µm</p> <p>UHV = 20.00 kV WD = 7.9 mm</p> <p>Signal A - SE2 Mag = 1.00 K X</p> <p>Date: 16 Aug 2011 Time: 16:00:54 Universiti Teknologi PETRONAS</p>



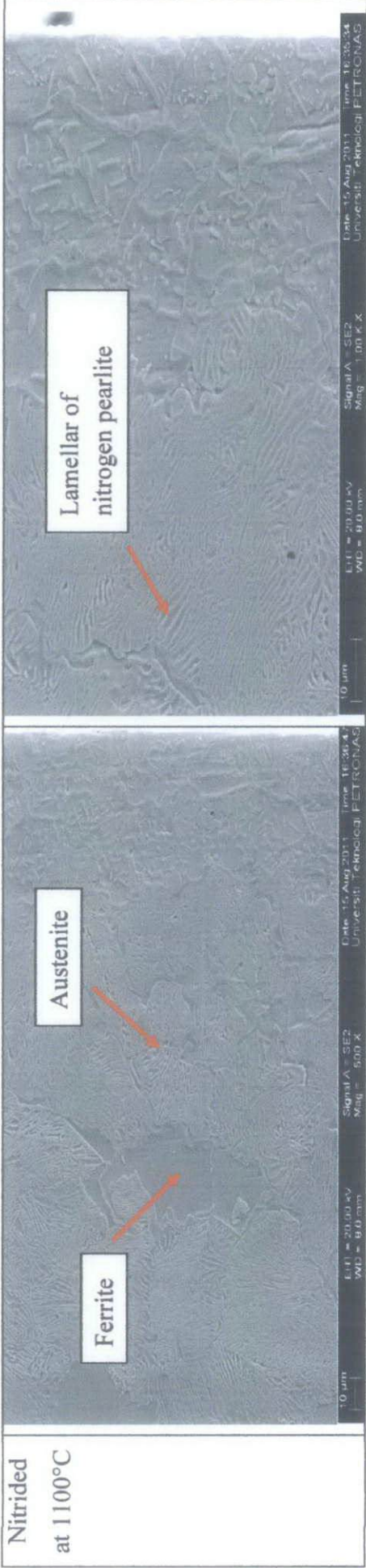


Figure 27: SEM microstructure images at various temperatures : unnitrided, 950°C, 1000°C, 1050°C and 1100°C

4.4.2 Microstructure Images by Optical microscope (OM)

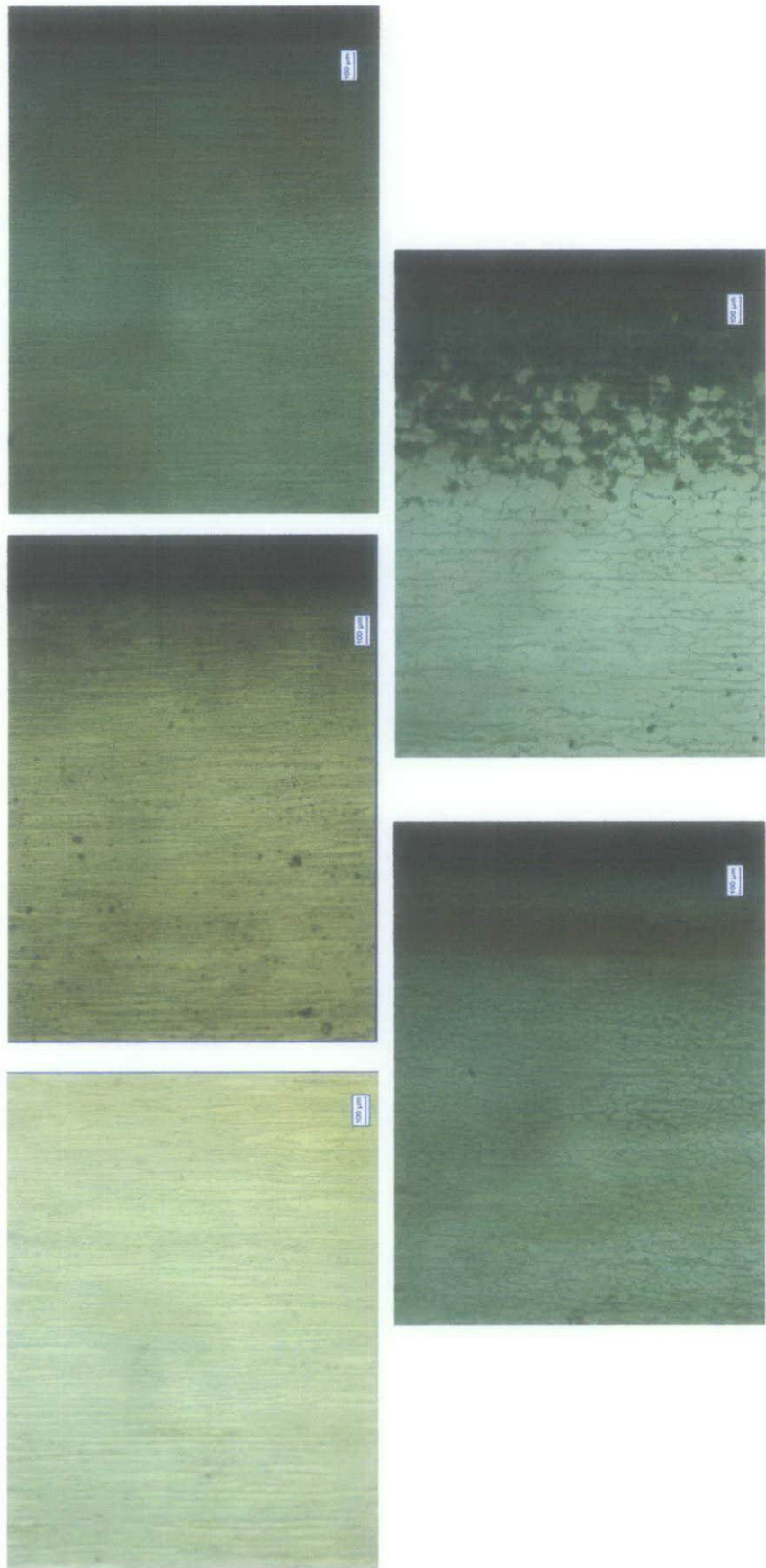


Figure 28: OM images of unnitrided sample and nitrided samples at temperatures of 950°C, 1000°C, 1050°C and 1100°C

The microstructure from Figure 27 and Figure 28 show the variation or changes of microstructure images from unnitrided to the nitrided at temperatures of 950°C, 1000°C, 1050°C and 1100°C. From all the microstructures images, there was no significant nitrided layer can be observed. Therefore, the author concluded that there was no diffusion zone in term of case depth that specifically shows the spot at which nitrogen is diffused interstitially for all the nitrided samples at high temperatures. This is contradictory with the result of microstructures conducted at low temperatures nitriding which the diffusion zone can be clearly seen [25].

From the SEM result, the unnitrided microstructure shows a fine distribution of ferrite and austenite over the whole cross section and some segregation bands in transverse direction. The grain boundaries are clean, straight and thin but no precipitates are observed in the microstructure. The ferrite phase is identified as darker phase while austenite is brighter phase. The microstructure of nitrided samples also consisted of about equal fractions of ferrite and austenite. This has not changed in the core after nitriding and only a slight increase of average grain size was registered which changes from the unnitrided samples until nitrided samples at 950°C and 1000°C. The sample at 1050°C and 1100°C shows a significant increase in the average grain size especially increases of size of austenite phase. This is due to the diffusion of nitrogen is higher in the austenite phase.

From the SEM and OM images, nitrided sample at 950°C have start induced the precipitates, the same as in the nitrided samples at 1000°C, 1050°C and 1100°. It was clearly seen in the OM microstructure image which the dark spots were observed at four nitrided samples. This is due to the higher nitrogen saturation on the austenitic matrix which becomes the driving force for iron and chromium nitrides precipitation. In Figure 27 and Figure 28 of nitrided sample at 1100°C, to the right of the image, show the increase of nitrogen and reduce the content of ferrite phase, so that austenite phase prevailed until a nitrogen content above solubility provoked the precipitation of nitrides along grain boundaries and closer to the surface, even in a lamellar form within some grains. The nitrides were identified by X-ray and electron diffraction in the next part as hexagonal  $M_2N$  nitrides where M means the main alloying mixture of elements of steels such as Cr and Fe that induced  $(Cr,Fe)_2N$ ,  $FeN$  and  $Fe_3N$ . Discontinuous cellular precipitation of  $M_2N$  proves to be a complex

precipitation phenomenon. As the morphology of the cellular precipitation is similar to that of pearlite in carbon steels, this kind of precipitation is often called as 'nitrogen pearlite' which is misleading, because the matrix between the nitride lamellae remains austenitic. During nitriding, the grain growth was impeded by the two-phase microstructure of the austenite and  $M_2N$  and the austenite and ferrite range. In the homogeneously austenitic range, the grain size was larger by a factor of 2-3. Such evidence can be seen and observed where a discontinuous precipitation (cellular phase transformation) appeared in lamellar or dispersed form (nitrogen pearlite) within austenite grains shown in SEM image at 1100°C. Not only that, from Figure 28 shows that a number of densely located precipitates were observed at the dark layer of the outmost surface of nitride sample at 1100°C in comparison which indicated  $M_2N$  in the form of  $(Cr,Fe)_2N$ ,  $FeN$  and  $Fe_8N$  have precipitated in agreement with the XRD result later.

The nitrogen diffused into the steel layer and precipitates on cooling to form nitrogen pearlite. As the author has conducted slow cooling process after performed the nitriding treatment, this could be the reason of such chromium nitrides and iron nitride precipitated and finally formed nitrogen pearlite. This is because, isothermal heat treatments of transformation in the temperature range of 700°C-900°C also cause chromium nitride precipitation in duplex stainless steel [3]. Therefore, to be related with such theory, the nitriding temperature at 950° has an advance of 50° before the temperature start to cools down to the chromium nitride precipitation temperature to occur which is in the range of 900°C. Compare with at nitriding temperature of 1100°C which the temperature is higher before reaching the precipitation range temperature. This is aligned with the theory that at higher temperature than the isothermal transformation temperature is allowed to occur, the diffusion rate are relatively high, such that during the transformation, more chromium and nitrogen atoms can diffuse relatively long distance which results in the formation of coarse lamellae of nitrogen pearlite as indicated in Figure 27. This is also evidence where pits were observed in OM images at temperatures 950°C, 1000°C, 1050°C and 1100° to initiate most commonly in the chromium-depleted matrix adjacent to chromium nitride precipitates in the samples.

#### **4.4.3 EDX Analysis – Line scan nitrogen profile**

The variations of chemical concentration of the interstitial element of nitrogen in the outmost surface of the samples were measured with Energy Dispersive Spectroscopy (EDS) line scan mode. Figure 29 below shows the typical nitrogen profiles produced in the sample of nitrided duplex stainless steel. The line scan nitrogen profile is taken by considering the x-ray intensity in the unit of counts per second (cps) for any particular element to be measured in y-axis and distance from the outmost surface in unit of micrometer ( $\mu\text{m}$ ).

The trends of all four nitrided samples show the nitrogen peak give higher intensity as the temperatures increases. This is because, during the line scan profile is observed, the frame measured to be scanned and time taken for scanning were constant and fixed for about 300 frames taken in 300 seconds. Therefore, during this range of fixed frames measured and scanning times, the peaks of nitrogen profile for all nitrided samples were obtained.

As shown in Figure 29a) below, the nitrogen profile for sample nitrided at 950°C, the highest nitrogen peak were obtained at the surface and relatively unchanged until at 200 $\mu\text{m}$  from surface. This proves that the distribution of nitrogen diffused interstitially almost equally to the surface of the samples up to 200 $\mu\text{m}$ . There is an improvement as the temperature increase to 1000°C, 1050°C and 1100°C where a significant increases of the nitrogen peak. From Figure 29b), c) and d) it show that the high peak of nitrogen is obtained at the outmost surface. The highest peak of intensity of nitrogen is obtained at temperature 1100°C which is approximately 21cps followed at 1050°C which is about 18cps. While at temperature 1050°C the intensity of nitrogen peak shows the value 15 cps and for nitrided sample at temperature 950°C, the lowest peak of nitrogen intensity is obtained at 8 cps. Therefore, it could be concluded that the intensity of nitrogen is observed to be increased as the temperature increased and in line with the agreement to the theory that mentioned the variation of temperatures at constant time does give a significant effect to the diffusion of nitrogen into the steel surface.



samples. Furthermore, in Figure 31, 32 and 33, the nitrogen composition were also detected and the value were kept increasing as the temperature increase On the other hand, the composition of chromium, Cr and iron, Fe in all the nitrated samples were decreased from the unnitrated samples. There were decreased gradually as the temperature increased. The depletion of element chromium and iron is in agreement with the precipitation of nitrides which formed the nitrogen pearlite especially in nitrated sample at temperature 1100°C. The figures below show the result of area analysis that the author obtained for unnitrated sample and all nitrated samples while the tables below show the quantitative result for unnitrated and all nitrated samples.

For unnitrated sample

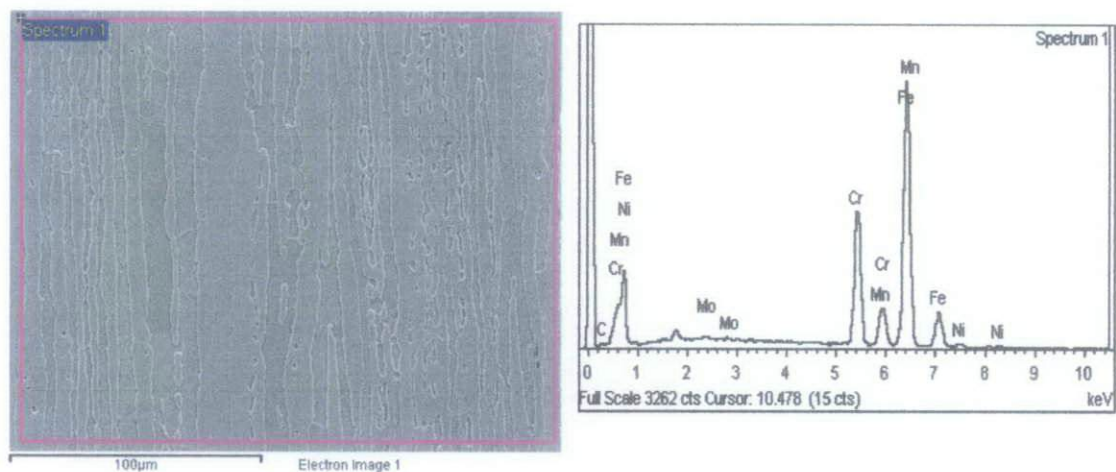


Figure 30: Image and qualitative result of unnitrated sample

Table 6: Quantitative result

Element	Cr	Mn	Fe	Ni	Mo
Weight %	22.74	5.77	72.17	1.94	0.10



For nitrided sample at 950°C

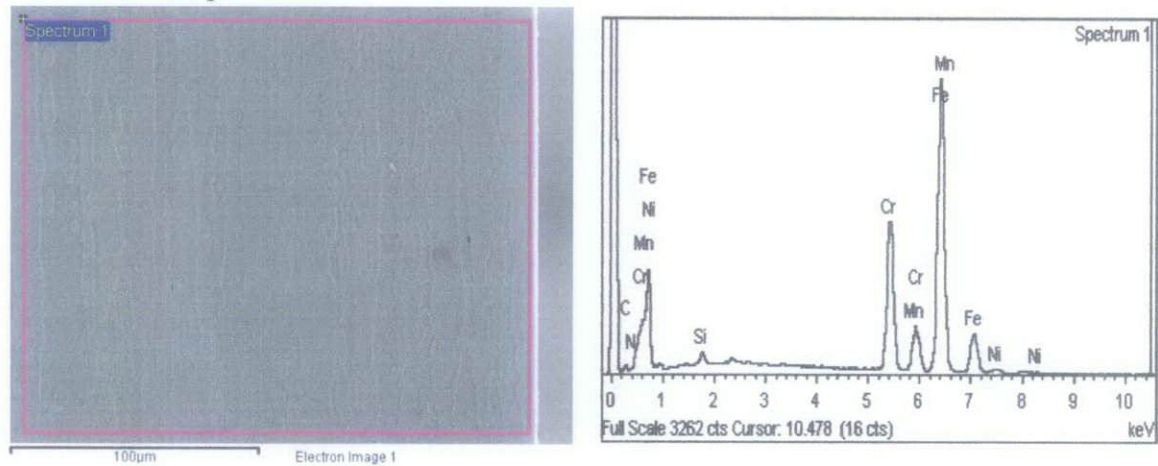


Figure 31: Image and qualitative result of nitrided at 950°C

Table 7: Quantitative result

Element	N	Si	Cr	Mn	Fe	Ni
Weight %	0.66	0.79	21.96	5.07	66.71	1.34

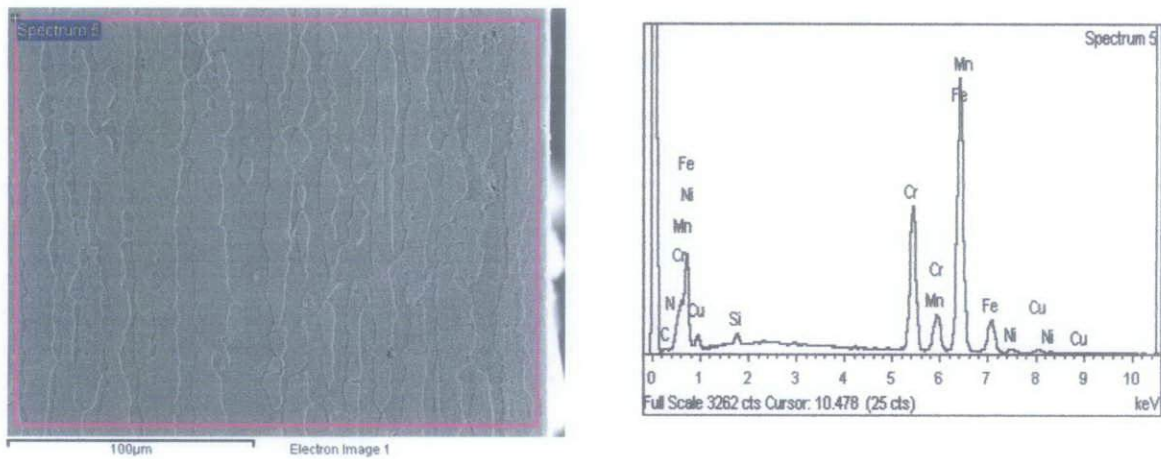


Figure 32: Image and qualitative result of nitrided at 1000°C

Table 8: Quantitative result

Element	N	Si	Mn	Cr	Fe	Ni	Cu
Weight %	1.44	0.83	3.82	21.48	66.45	1.49	0.88

For nitrided sample at 1050°C

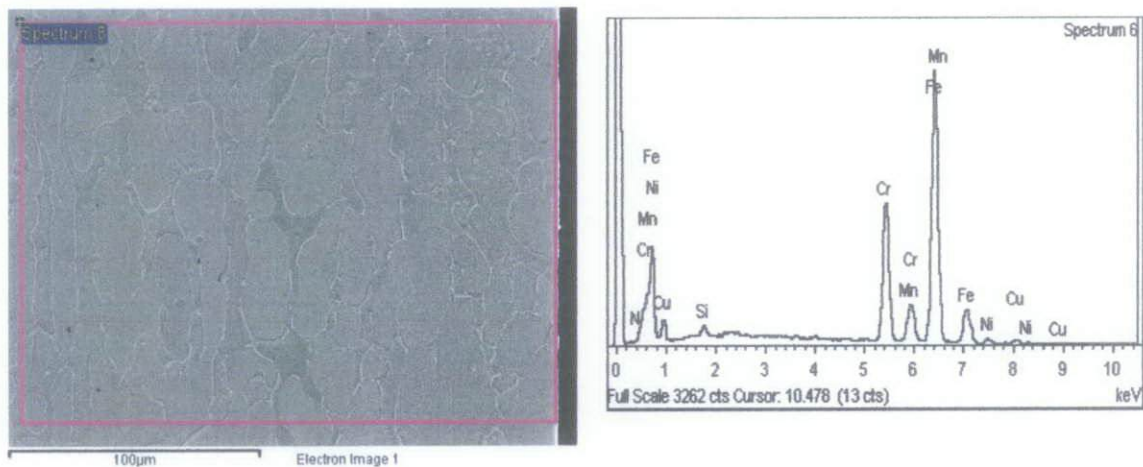


Figure 33: Image and qualitative result at 1050°C

Table 9: Quantitative result

Element	N	Si	Cr	Mn	Fe	Ni	Cu
Weight %	1.97	2.38	21.43	5.04	64.69	1.74	2.75

For nitrided sample at 1100°C

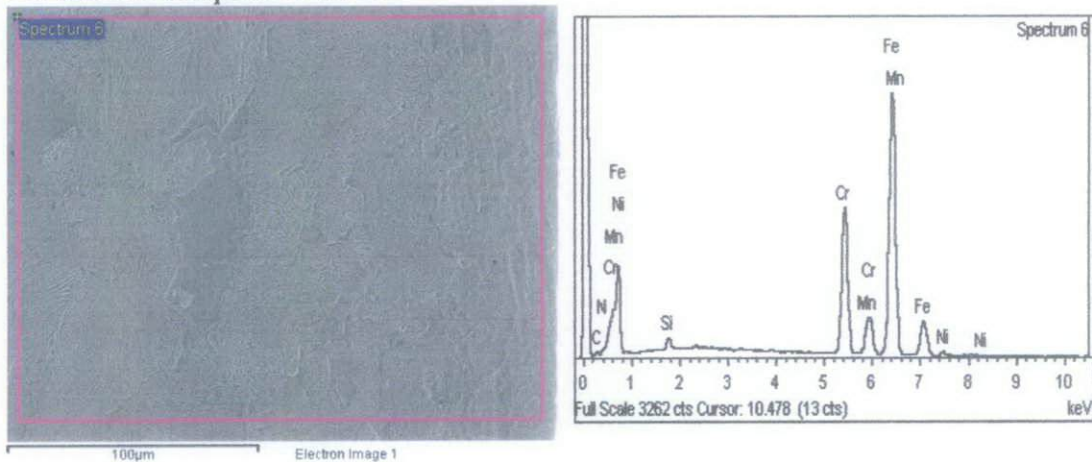


Figure 34: Image and qualitative result of nitrided at 1100°C

Table 10: Quantitative result

Element	N	Si	Cr	Mn	Fe	Ni
Weight %	2.82	0.99	21.31	4.87	64.03	1.50

#### 4.4.5 EDX Analysis - Spot Analysis

For this part, the author has conducted a spot analysis using energy dispersive x-ray analysis (EDX). The purpose of this particular analysis is to analyze whether the interstitial element of nitrogen were highly diffused in austenite phase or in ferrite phase. As have been mentioned in the literature, element nitrogen is a strong austenite former and stabilizer. Therefore, from this spot analysis could be an evidence to prove such information.

Previously, the author have mentioned that the austenite phase is marked as brighter in colour while ferrite phase is more darker in colour. Therefore, from the Figure 35 for unnitrided sample, there were no nitrogen detected in both austenite and ferrite phase. This is tolerable since this sample is not undergoing nitriding yet and as have been proven in area analysis before, which there was no nitrogen detected at all.

In addition, as shown in Figure 36 and Table 13 and 14, the weight percentage of nitrogen is given a markedly value in austenite phase compare in ferrite phase. This is evidence that nitrogen is diffused interstitially in austenite phase which resulted in higher value of nitrogen weight percentage at that particular phase.

This is contradictory with the pattern of nitrogen diffusion in nitrided sample at 950°C compare to the other nitrided samples where there were significant amount of nitrogen diffused in both austenite and ferrite phase for nitrided samples at 1000°C, 1050°C and 1100°C as have shown in Figure 37, 38, 39 and their respective quantitative results. However, the weight percentage of nitrogen that diffused interstitially in austenite phases still gives a higher percentage compare to ferrite phases. This is according to the theory which the nitrogen diffusion is more preferable in austenite phases. Not only that, the weight percentage of chromium and iron at austenite and ferrite phases also seem to be decreased from the unnitrided sample of austenite and ferrite phases as in line to the result that precipitation of chromium and iron nitrides gives a markedly decrease value to that particular elements. The nitrides are high in Cr, N, and Fe which caused a respective depletion of the adjacent matrix. However, the chromium and iron elemental composition at austenite and ferrite for four nitrided samples were not decreased gradually. The



author observed that, although the decreasing of element chromium and iron were not steadily as the nitriding temperature increases but the weight percentage of those elements were decreased more within austenite phases and due to the precipitates of nitrides were mostly propagate within the austenite phases as in agreement with the result shown from x-ray diffraction (XRD) analysis later. Figures and tables below show the spot analysis results.

For unnitrided sample

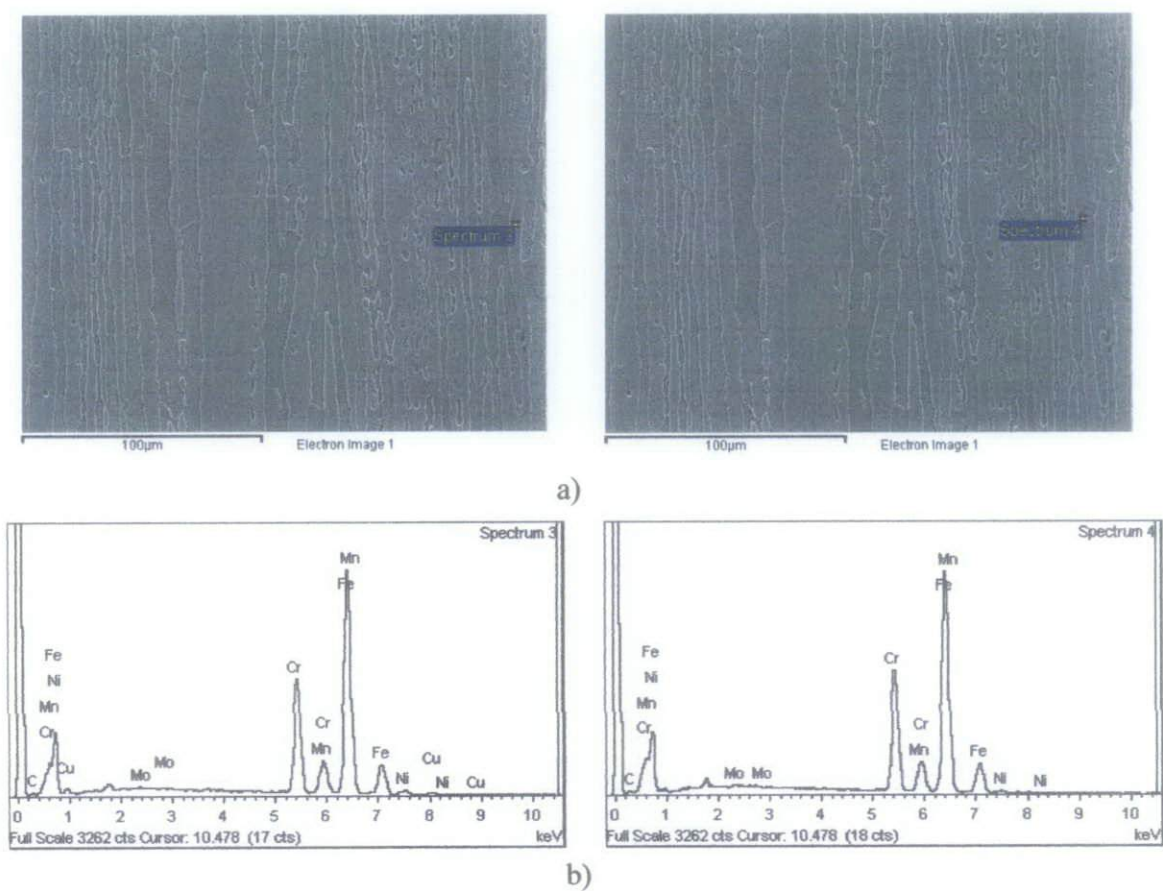


Figure 35: a) Image of spectrum 3 and spectrum 4, b) Qualitative result

Table 11: Spectrum 3 of austenite phase

Element	Cr	Mn	Fe	Ni	Cu	Mo
Weight %	24.81	5.44	75.30	1.81	0.93	0.26

Table 12: Spectrum 4 of ferrite phase

Element	Cr	Mn	Fe	Ni	Mo
Weight %	24.04	5.01	73.46	1.07	0.54

For nitrated sample at 950°C

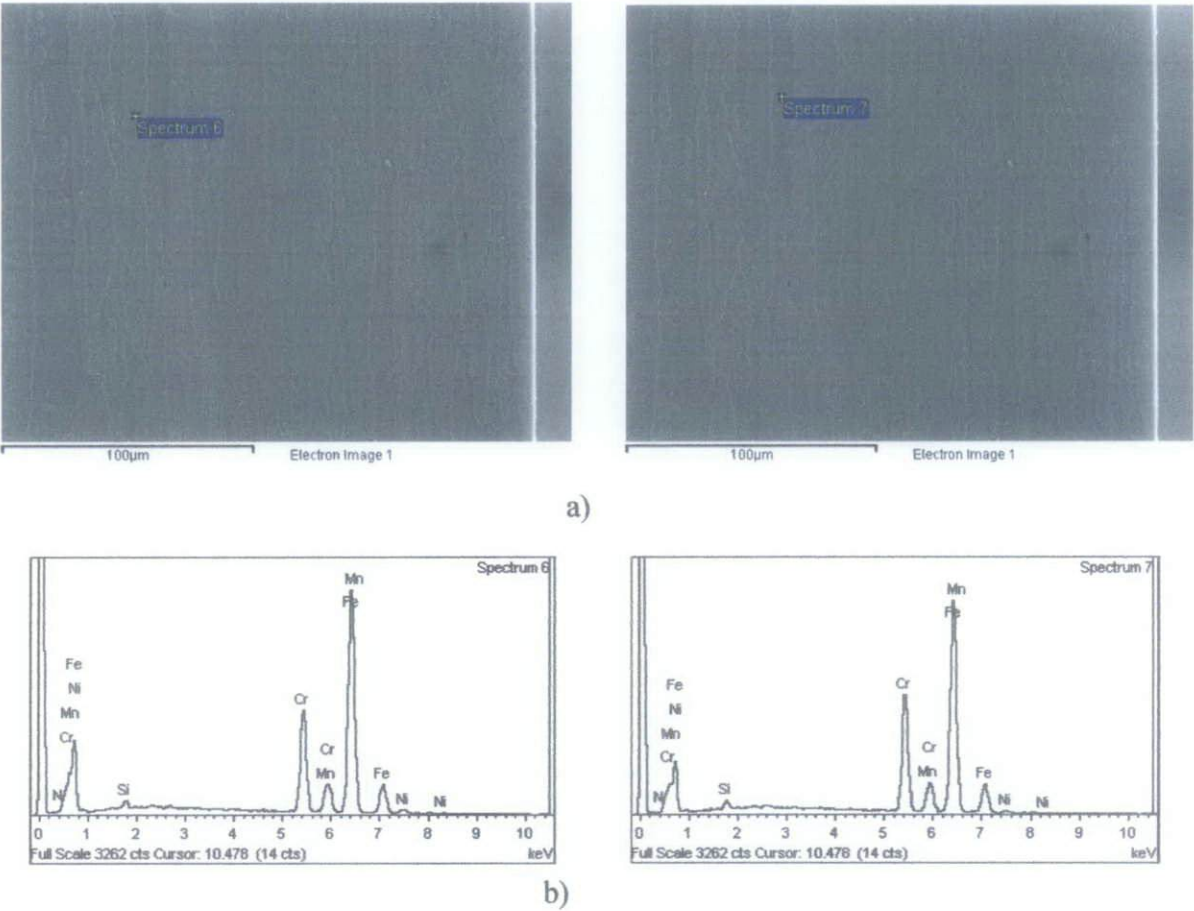


Figure 36: a) Image at spectrum 6 and spectrum 7, b) Qualitative result

Table 13: Spectrum 6 on austenite phase

Element	N	Si	Cr	Mn	Fe	Ni
Weight %	0.29	0.75	21.87	5.59	69.96	1.54

Table 14: Spectrum 7 on ferrite phase

Element	N	Si	Cr	Mn	Fe	Ni
Weight %	0.52	0.84	23.57	4.56	70.14	1.41

For nitrated sample at 1000°C

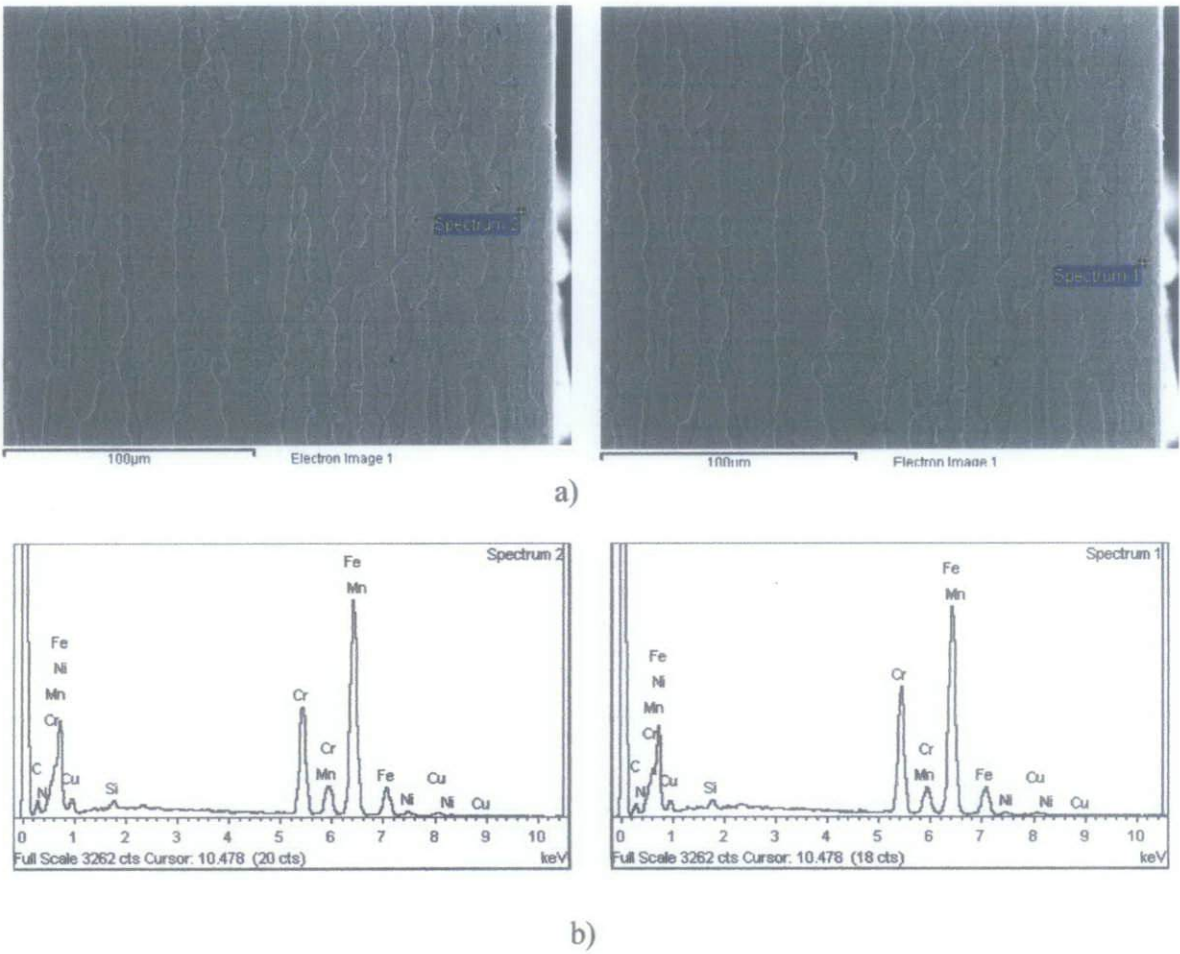


Figure 37: a) Image of spectrum 2 and spectrum 1, b) Qualitative result

Table 15: Spectrum 2 on austenite phase

Element	N	Si	Cr	Mn	Fe	Ni	Cu
Weight %	1.38	0.61	18.80	4.43	60.1	1.38	1.29

Table 16: Spectrum 1 of ferrite phase

Element	N	Si	Cr	Mn	Fe	Ni	Cu
Weight %	0.56	0.99	22.56	3.79	63.04	1.00	0.52

For nitrated sample at 1050°C

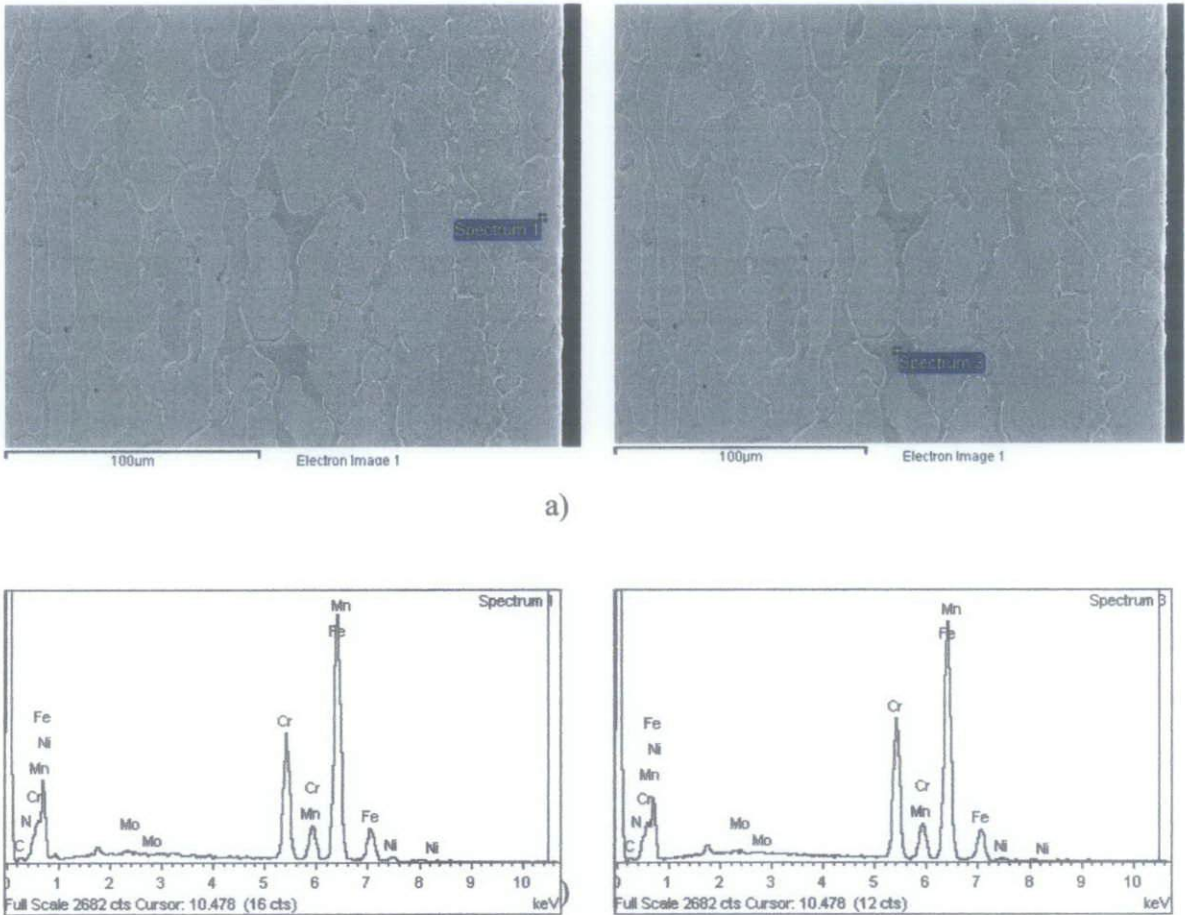


Figure 38: a) Image at spectrum 1 and spectrum 3

Table 17: Spectrum 1 on austenite phase

Element	N	Cr	Mn	Fe	Ni	Mo
Weight %	1.52	22.00	4.67	70.77	1.69	0.74

Table 18: Spectrum 3 on ferrite phase

Element	N	Cr	Mn	Fe	Ni	Mo
Weight %	1.14	23.45	4.66	70.98	1.78	0.53



For nitrided sample at 1100°C

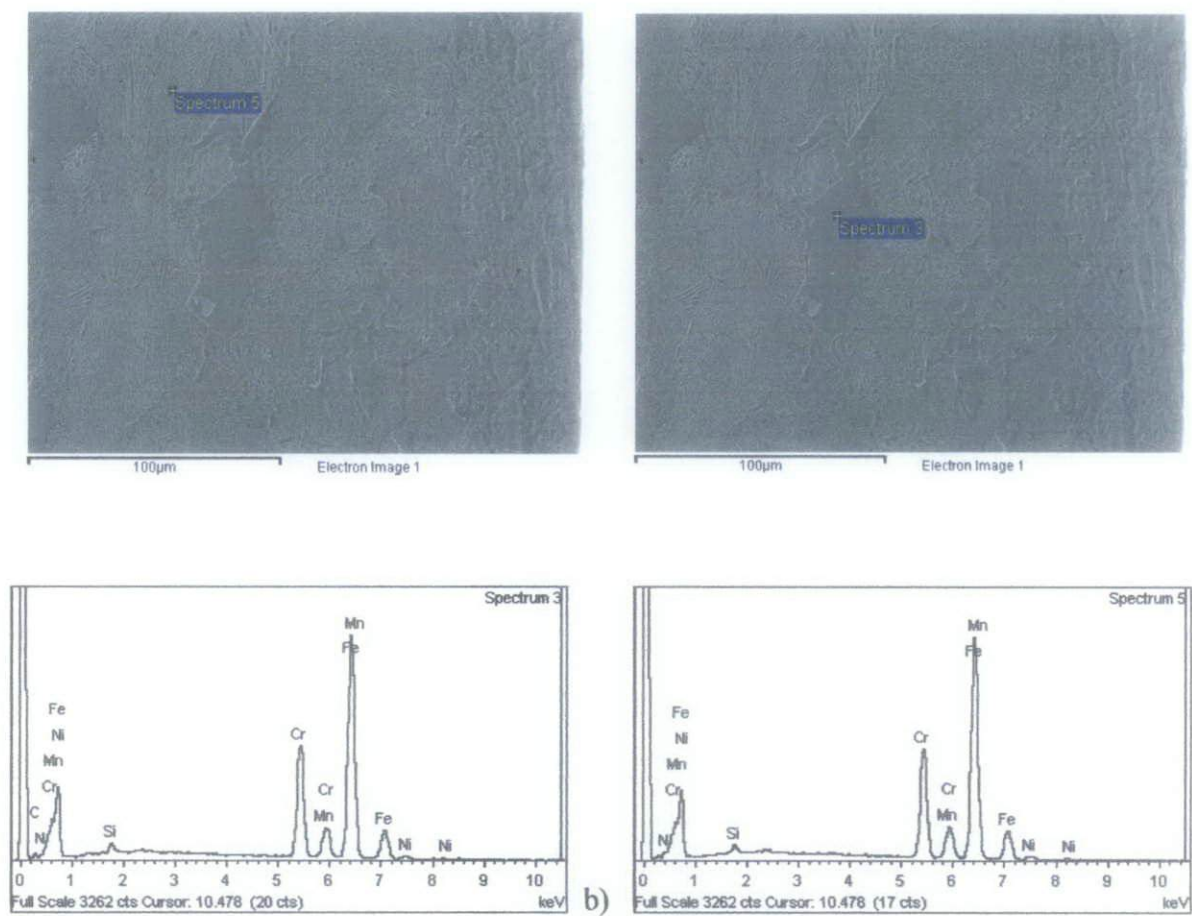


Table 19: Spectrum 3 of austenite phase

Element	N	Si	Cr	Mn	Fe	Ni
Weight %	2.01	0.68	20.92	5.11	69.65	1.63

Table 20: Spectrum 5 at ferrite phase

Element	N	Si	Cr	Mn	Fe	Ni
Weight %	1.74	0.90	21.08	3.12	69.78	1.27



For nitrated sample at 1050°C

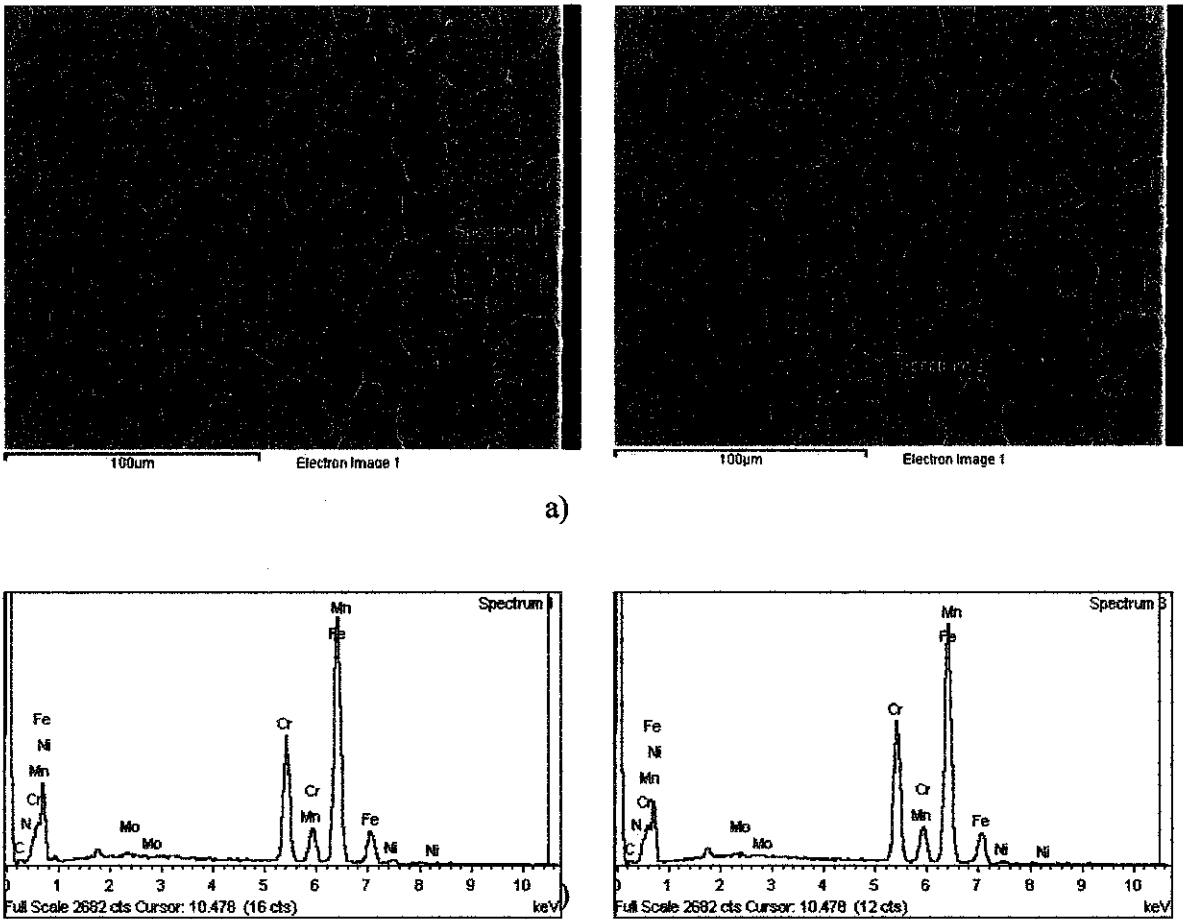


Figure 38: a) Image at spectrum 1 and spectrum 3

Table 17: Spectrum 1 on austenite phase

Element	N	Cr	Mn	Fe	Ni	Mo
Weight %	1.52	22.00	4.67	70.77	1.69	0.74

Table 18: Spectrum 3 on ferrite phase

Element	N	Cr	Mn	Fe	Ni	Mo
Weight %	1.14	23.45	4.66	70.98	1.78	0.53

For nitrided sample at 1100°C

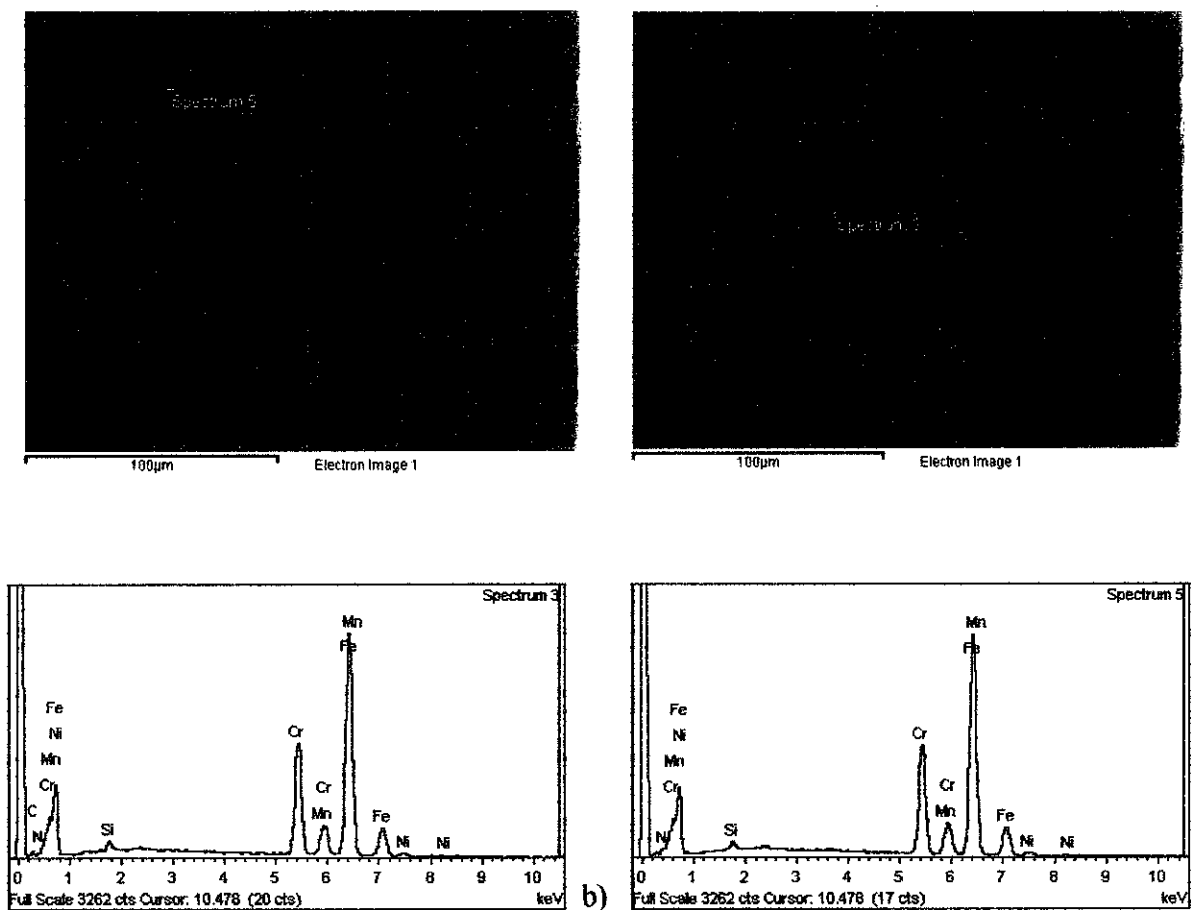


Table 19: Spectrum 3 of austenite phase

Element	N	Si	Cr	Mn	Fe	Ni
Weight %	2.01	0.68	20.92	5.11	69.65	1.63

Table 20: Spectrum 5 at ferrite phase

Element	N	Si	Cr	Mn	Fe	Ni
Weight %	1.74	0.90	21.08	3.12	69.78	1.27

#### 4.4.6 X-ray Diffraction Analysis

In order to clearly demonstrate which phases appeared at the surfaces of the unnitrided and nitrided samples, x-ray diffraction (XRD) measurement was employed. Phase identification on virgin austenite and ferrite on the nitrided layer were performed by X-ray diffraction (XRD) using Cu-K $\alpha$  radiation. As shown in figure below the patterns of the unnitrided samples and nitrided samples. The unnitrided sample showed a mixed structure of ferrite and austenite. This result for the unnitrided sample was in line with the X-Ray Diffraction pattern for untreated sample of duplex stainless steel in the literature which showed the austenite- $\gamma$  peak and ferrite- $\alpha$  peak were at the same glancing angle as the pattern that the author obtained. The surface of the nitrided samples consisted of ferrite, austenite, chromium nitrides and iron nitrides.

After nitriding at 950°C, the presence of nitrides predominates. At this nitriding temperature, chromium nitrides (Cr,Fe) $_2$ N in the unit cell of primitive hexagonal structure was detected at angle of 43° of the sample surface. Next, at this nitriding temperature two types of iron nitrides were also detected. At glancing angle of 44°, iron nitrides ( $\gamma'$ -FeN) as in cubic unit cell while at angle of 45°, nitrides that appeared was ( $\alpha'$ -Fe $_8$ N) in the form of tetragonal structure also detected. According to the chemical composition of this duplex stainless steel Fe and Cr are expected to be dissolved in iron and chromium nitrides, but nitrides stoichiometry can not be evaluated in the present analysis. As a consequence of the high nitrogen pick-up on these nitrides, its fraction increases with increasing nitrogen content as the nitriding temperature increases.

Furthermore, as can be seen in the figure below, the (Cr,Fe) $_2$ N, ( $\gamma'$ -FeN) and ( $\alpha'$ -Fe $_8$ N) peaks were observed along with the  $\alpha$  and  $\gamma$  peaks. It is believed that the appearance of these precipitates was due to the affinity between chromium and iron with nitrogen. The peak of (Cr,Fe) $_2$ N detected for nitrided sample at temperature 950°C but its gives the lowest intensity compared to the other nitrided samples. As the temperature increase, the peak of (Cr,Fe) $_2$ N was getting higher except at nitriding temperature of 1050°C, the particular peak drops intensely. However, there was

another peak of  $(\text{Cr,Fe})_2\text{N}$  was detected at glancing angle  $56^\circ$  of the sample surface at this nitriding temperature. There was an improvement as the temperature increase to  $1100^\circ\text{C}$  where the peaks intensity for this chromium nitride precipitates,  $(\text{Cr,Fe})_2\text{N}$  were getting higher and predominates compared to other nitriding temperatures. Not only that, as can be observed at all the nitrided samples, iron carbides in the form of  $\alpha'$ - $\text{Fe}_8\text{N}$  and  $\gamma''$ - $\text{FeN}$  were detected. These iron nitrides were originally from the peak of  $\alpha$  and  $\gamma$ . These could be concluded that,  $\alpha'$ - $\text{Fe}_8\text{N}$  nitrides were form in the lattice of body-centered cubic (bcc) as explained the ferrite crystal structure while  $\gamma''$ - $\text{FeN}$  nitride in the lattice of face-centered cubic as explained the austenite crystal structure. As far as the author concern, when more than 2.4 at %N (nitrogen) is dissolved in pure Fe, the bcc lattice undergoes tetragonal deformation which resulted  $\alpha'$ - $\text{Fe}_8\text{N}$  nitride. In this composition range up to about 11 at % N, the iron nitride compound is also called nitrogen martensite  $\alpha'$ . This phase has a body centered tetragonal (bct) structure with lattice parameter depending on the nitrogen content. The nitrogen (N) atoms occupy randomly octahedral hollow sites in the Fe sublattice.

Furthermore, for the case of  $\gamma''$ - $\text{FeN}$  phase which is cubic, with the Fe-sublattice arranged in a face-centered cubic (fcc) structure. This type of phase was detected at all the nitrided samples. This phase is predicted to have even more nitrogen (N) rich compounds. The theoretical prediction of this phase was made following the prediction and subsequent experimental confirmation of other MN compounds (M=metal, N=nitrogen). This phase was predicted to have a nitrogen content of 50 at % nitrogen (N) but with different configuration of the N atoms within the fcc Fe cage. The co-existence of this type of phase is still a matter of controversy and its behaviour is still under discussion. However, as been mentioned that this phase was forecasted to have higher amount of nitrogen content and this is in line with the result that the author gained from EDX area and spot analysis which stated that, as the temperature increases, the nitrogen content that diffused to the steel surface also increases. The precipitates detected were also the main factors contributed to the surface hardening of the metal as the hardness values at surface of the nitrided samples were markedly increases. The figure below showed the XRD result that the author gained.

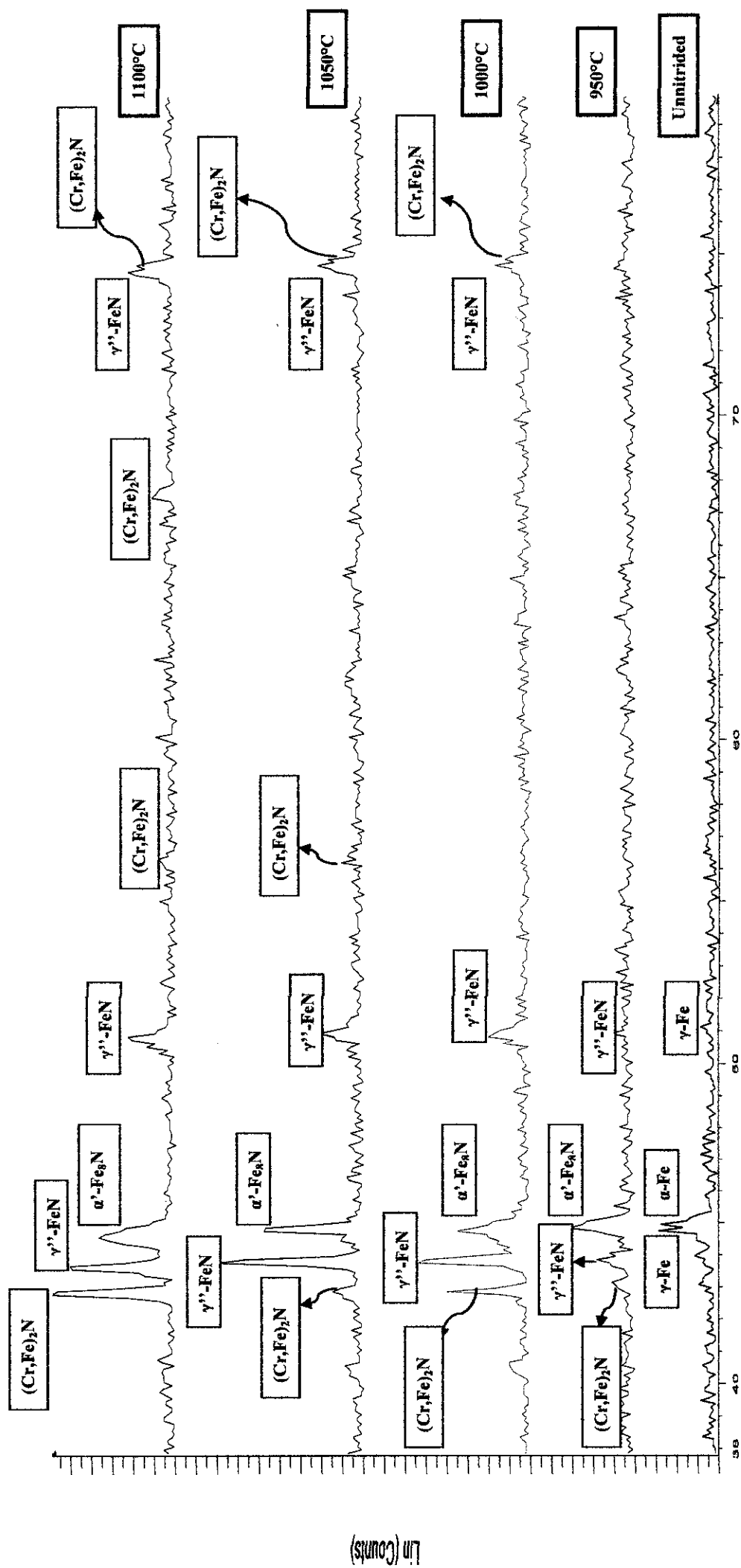


Figure 40: XRD patterns for duplex stainless steel of unnitrided sample and nitrided samples

## **CHAPTER 5: CONCLUSION & RECOMMENDATION**

### **5.1 Conclusion**

As a conclusion, the objectives set up for this research has been accomplished which are basically to investigate the effect of nitriding temperature towards the mechanical properties of the duplex stainless steel. The high temperature gas nitriding has successfully improved the surface of the duplex stainless steel.

As the temperature increases, it improves the hardness of the steel due to the diffusion of nitrogen into the steel. Highest hardness; 448.2HV is achieved by sample nitrided at 1100 °C for six hours. Not only that, the microstructures of the nitrided samples also were observed to have some changes due to the nitriding and cooling process that all the samples experienced. There was also significance difference with the unnitrided sample.

Furthermore, correlated to the temperature changes, the microstructures were undergoing transformations to new phases which in this case, the nitrides formed and resulted to the hardening of the metal surface as the hardness were increased.

In general, types of the nitrides that formed were proved by the x-ray diffraction analysis. There were three types of nitrides that formed and can be observed in the microstructures that eventually assisted to the surface hardening of this type of steel.

Last but not least, with all the results that the author obtained, it can be concluded that, the nitriding temperatures did gave the major effects to the hardness measurement, microstructure changes of this type of duplex stainless steel. As the temperature increases, the hardness values of samples were also increased. Not only that, when the temperature increases, the microstructures also experienced major changes from the nitriding process. Therefore, the objectives of this work have been achieved successfully.

## **5.2 Recommendation**

For future research, some improvements could be done. It is recommended for future investigations to:

- i. Examine the elements and phases exist in nitrided samples thoroughly to provide further details on the microstructural behavior and strengthening effects.
- ii. Measurement on nitrogen content at the treated samples is required to relate the hardness of the treated sample by using Glow Discharge Spectroscopy
- iii. Identify the optimum parameters such as the compaction pressure and most suitable nitriding temperature and time to improve the properties of the steel.
- iv. In future, the tensile testing is recommended to be performed to prove and achieve the expectation of enhancing the ductility.

## REFERENCES

- [1] Robert N Gunn on “Duplex Stainless Steels: Microstructure, properties and applications” by Abington Publishing of Cambridge England.
- [2] U. Kamachi Mudali, Baldev Raj 2004, High Nitrogen Steels and Stainless Steels Manufacturing Properties and Application, India, Narosa Publishing House, New Delhi
- [3] William D.Callister, Jr 2003, Materials Science and Engineering, an Introduction, United States of America, John Wiley & Sons
- [4] International Molybdenum Association on “Practical Guideline for the Fabrication of Duplex Stainless Steels “, Second Edition on 2009.
- [5] <http://www.rolledalloys.com/trc/viewdoc.aspx?n1=corrosion&n2=idx>, Title: *Data Sheet of LDX2101 Duplex Stainless Steel*, accessed date: 13 September 2010
- [6] Hudiyo Firmanto, Patthi Hussain, Othman Mamat on “*Solution Nitriding of AISI 430 Ferritic Stainless Steel*” Mechanical Engineering Department, Universiti Teknologi PETRONAS, Tronoh, Perak (2009)
- [7] Kimiaki Nagatsuka, Akio Nishimoto, Katsuya Akamatsu on “ *Surface hardening of duplex stainless steel by low temperature active screen plasma nitriding*” Surface & Coating Technology (2010)
- [8] E.Erisir, U. Pahl and W. Bleck on “*Effect on precipitation on hot formability of high nitrogen steels*” Department of Ferrous Metallurgy, RWTH Aachen University, Germany (2010)
- [9] F.Shi, L.J. Wang, W.F. Cui, and C.M. Liu on “ *Precipitation Behavior of  $M_2N$  in a High-Nitrogen Austenitic Stainless Steel During Isothermal Aging*”, School of Materials & Metallurgy, Northeastern University, Shenyang 110004, China (2007)
- [10] J.H. Kong, D.J. Lee, H.Y. On, S.H.Lee, J.H.Sung, and H.W. Lee on “*The Characteristic of High Temperature Gas Nitriding Heat Treatment and Tempering in 0.8Mo Added 17Cr-1Ni-0.5C*”, Department of Materials Science
- [11] Tomonori Nakanishi, Toshihiro Tsuchiyama, 2007, “*Effect Of Partial Solution Nitriding On Mechanical Properties And Corrosion Resistance In A Type 316L Austenitic Stainless Steel*”, Material Science and Engineering A: 460-461 (2007) 186-194
- [12] José Francisco, Carlos Mario and André Paulo, *Improvement of the cavitation erosion resistance of an AISI 304L austenitic stainless steel by high temperature gas*



*nitriding*, Material Science and Engineering A, Volume 382, 25 September 2004, Pages 378-386

[13] K.Y. Li and Z.D. Xiang, 2010, "*Increasing Surface Hardness Of Austenitic Stainless Steel By Pack Nitriding Process*", Surface and Coatings Technology: xxx (2010) xxx-xxx

[14] Donald C. Zipperian, Ph.D, Pace Technologies, manual on *XRD Conversion User Manual*

[15] *Manual on Metallographic Sample Preparation*, Material Laboratory Universiti Teknologi Petronas, Department of Mechanical Engineering (2004)

[16] J.H.Sung, J.H.Kong, D.K.Yoo, H.Y.On, D.J.Lee, H.W.Lee, 2007, "*Phase Changes of the AISI 430 Ferritic Stainless Steels after High-Temperature gas nitriding and tempering Heat Treatment*", "Department of Materials Science and Engineering, Dong-A University, 840 Hadan-dong, Saha-gu, Busan 604-714, Republic of Korea, "Material Science and Engineering A-489(2008) 38-43

[17] D.K. Yoo, H.J. Lee, C.Y. Kang, K. H. Kim, Y.H. Kim, and J.H. Sung, Solid State Phenomena 118, 149 (2006)

[18] E. Folkhard, *Welding Metallurgy of Stainless Steel*, 1<sup>st</sup> ed, p. 103, Springer, New York (1986)

[19] <http://www.materials.co.uk/vickers.htm>, Title: *Vickers Hardness Test*, accessed date: 2 October 2010

[20] [www.heattreatnews.com/pdf/NitridingKnowledgeArticle.pdf](http://www.heattreatnews.com/pdf/NitridingKnowledgeArticle.pdf) Title: *Nitriding Knowledge*, accessed date: 8 September 2010

[21] C.M Garzon, A.P Tschiptschin, *Processing of The International Conference on High Nitrogen Steels 2004*, GRIPS media GmbH, Bad Harzburg, 2004, pp. 205-213

[22] Hans Berns, Andreas Kuhl on "*Reduction in Wear of Sewage Pump through Solution Nitriding*", from Institut for Werkstoffe, Ruhr Universitat Bochum, Lehrstuhl Werkstofftechnik, Bochum I D-44780, Germany (2004)

[23] C.M. Garzon on "*EBSD texture analysis of high temperature gas nitride duplex stainless steel*", Metallurgical and Materials Engineering Department, University of Sao Paulo (USP), Brazil (2006)

[24] P.Hussain, O.Mamat, M.Mohammad and W.M.N. Wan Jaafar on "*Formation of Nitrogen Pearlite in the Dissusion Bonding of Sialon to 316L Stainless Steel*", Department of Mechanical Engineering, Universiti Teknologi PETRONAS, Perak (2010)

- [25] A.Triwiyanto, P.Hussain, M.Che Ismail on “ *Behavior of carbon and Nitrogen after Low Temperature Thermochemical Treatment on Austenitic and Duplex Stainless Steel*”, Department of Mechanical Engineering, Universiti Teknologi PETRONAS (2010)
- [26] ASTM E-92-82 ( Reapproved 1997), “ *Standard Test Method for Vickers Hardness of Metallic Materials*”, Copyrighted by ASTM, 100 Bar Harbor Drive, PO Box C700, Wesr Conshohocken, PA 19428-2959, United States.

## APPENDIX



Figure i : The samples before being cut at cross section

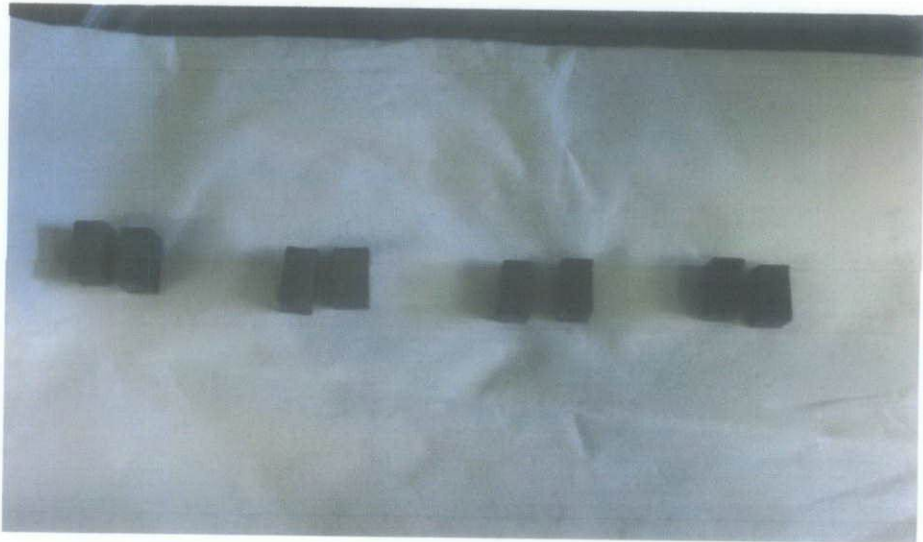


Figure ii: The samples after being cut